Identification of Highly Deformed Even-Even Nuclides in the Neutron- and Proton-Rich Regions of the Nuclear Chart from the $B(E2)\uparrow$ and $E2$ Predictions in the Generalized Differential Equation Model

R. C. Nayak

Department of Physics, Berhampur University, Brahmapur-760007, India.

and S. Pattnaik

Taratarini College, Purusottampur, Ganjam, Odisha, India.

Abstract

We identify here possible occurrence of large deformations in the neutron- and proton-rich regions of the nuclear chart from extensive predictions of the values of the reduced quadrupole transition probability $B(E2)\uparrow$ for the transition from the ground state to the first 2^+ state and the corresponding excitation energy $E2$ of even-even nuclei in the recently developed Generalized Differential Equation model exclusively meant for these physical quantities. This is made possible from our analysis of the predicted values of these two physical quantities and the corresponding deformation parameters derived from them such as the quadrupole deformation β_2, the ratio of β_2 to the Weisskopf single-particle $\beta_{2(sp)}$ and the intrinsic electric quadruplole moment Q_0, calculated for a large number of both known as well as hitherto unknown even-even isotopes of Oxygen to Fermium (Z=8 to 100). Our critical analysis of the resulting data convincingly support possible existence of large collectivity for the nuclides $^{30,32}Ne$, ^{34}Mg, ^{60}Ti, $^{42,62,64}Cr$, $^{50,68}Fe$, $^{52,72}Ni$, $^{72,70,96}Kr$, $^{74,76}Sr$,$^{78,80,106,108}Zr$, $^{82,84,110,112}Mo$, ^{140}Te,^{144}Xe, ^{148}Ba, ^{122}Ce, $^{128,156}Nd$, $^{130,132,158,160}Sm$ and $^{138,162,164,166}Gd$, whose values of β_2 are found to exceed 0.3 and even 0.4 in some cases. Our findings of large deformations in the exotic neutron-rich regions support the existence of another "Island of Inversion" in the heavy-mass region possibly caused by breaking of the N=70 sub-shell closure.

PACS numbers: 21.10.-k

1 Introduction

Studies of the nuclear structure for nuclei lying away from the β-stable valley of the nuclear chart has been a challenging situation of late, due to new phenomena being observed such as the shell-quenching[1, 2] of the so-called magic shell gaps, and the onset of exotic deformations leading to the existence of the so-called "Island of Inversion"[3, 4, 5]. Improved experimental technology and increased accuracy of the necessary tools have provided the desired boost making feasible for such discoveries. More or less, such issues are associated with the onset of increased collectivity[6, 7] leading to possible occurrence of large deformations of those nuclei lying in the exotic regions of the nuclear chart. In this connection values of the physical quantities such as the reduced electric quadrupole transition probability $B(E2)\uparrow$ for the transition from the ground state to the first 2^+ state and the corresponding excitation energy $E2$ of even-even nuclei play very decisive role[8] in identifying such occurrences of increased collectivity. Particularly the resulting quadrupole deformation parameters β_2 and the ratio of β_2 to the Weisskopf single-particle $\beta_{2(sp)}$ derived from them significantly help in this regard. Over the years host of such experimental data for these two physical quantities have led Raman et al. [9] to undertake the well-known Oak-Ridge Nuclear Data Project [10] to make a comprehensive analysis of all such data leading to compilation of the desired adopted data table in the year 1987[10] and 2001 [9]. More recently Pritychenko et al. [11] have continued the same Oak-Ridge program in compiling the newly emerging data for even-even nuclei near $N \sim Z \sim 28$.

Thus the study of these two physical quantities $B(E2)\uparrow$ and $E2$ has been under constant investigation both by experimentalists and theorists. Several theoretical study of these quantities have been the epitome of various models and authors [see for instance Raman et al.'s [8] comprehensive analysis]. Global systematics particularly by Grodzins[12], Bohr and Mottelson [13] and Wang et al. [14] were quite useful in the past. However for local systematics of these quantities, models in terms of difference equations developed by Ross and Bhaduri [15] and by Patnaik et al. [16] were found to be successful to some extent. In this regard our recently developed differential equation model[17, 18] for the physical quantity $B(E2)\uparrow$ has been found to be quite successful. In fact we could later on succeed in extending [19] the same model to include its complementary physical quantity, namely the excitation energy $E2$. According to this model which we may term it as the Generalized Differential Equation (GDE) model, the value of both these quantities for a given even-even nucleus is expressed in terms of their derivatives with respect to the corresponding neutron and proton numbers N, Z. The same differential equation in the model has been further exploited to generate two recursion relations, which are mainly responsible for the success[17, 18, 19] of the model not only for fitting the known data, but also for predicting the unknown

when compared with the recently compiled experimental data of Pritychenko et al. [11] in the $N \sim Z \sim 28$ region. In passing, we may note that we[17, 19] could visualize such a differential equation for these quantities on the basis of their close similarity in reflecting the shell-structure with the so-called local energy of the Infinite Nuclear Matter (INM) Model[20, 21, 22, 23] of atomic nuclei developed over the years primarily based on the generalized[24] Hugenholtz-van Hove theorem[25] of many-body theory. It may be of interest to note that the form of the differential equation in the GDE model as well as for the local energy in the INM model are exactly similar to that of the generalized[24] HVH theorem of many-body theory. We may further stress here that any relation in the form of a differential equation for any physical quantity is intrinsically sound enough to possess the desirable feature of good predictive ability. In fact this was found to be true behind the success[23] of the INM model as a mass formula and also with the presently considered GDE model[17, 18, 19].

Here in the present work, we are particularly interested to focus possible occurrence of increased collectivity leading to identification of exotic deformations for the nuclides lying mostly in the neutron- and proton-rich (n-rich and p-rich) regions of the nuclear chart. This is achieved from our analysis of the widely predicted data made in our model for the two physical quantities $B(E2)\uparrow$ and $E2$, and from the deformation parameters calculated from them. Accordingly we used our model first, in predicting their values for most of the even-even isotopes lying in the nuclear chart from Z=8 to 100 (O to Fm) confined to the known data-set region of Raman et al. [9], and then to the adjacent isotopes for which such values are not yet experimentally available. Then in the second step, we utilized these predicted values in calculating the relevant deformation parameters, namely the quadrupole deformation β_2, the ratio of β_2 to the Weisskopf single-particle $\beta_{2(sp)}$, and the intrinsic electric quadrupole moment Q_0 following the usual model-dependent formalism, in which nuclei are treated as having uniform charge distributions. These calculations provide us the necessary tools to analyze our data in a better way in identifying possible occurrence of increased collectivity and the resulting exotic deformations.

In the following section 2, we first of all discuss our model in brief for sake of continuity and fruitful analysis of the resulting data. Section 3 deals with the usual details of calculation. Subsequently we present our results and discuss them in section 4. Finally we highlight our main findings in the concluding section 5.

2 The Generalized Differential Equation Model for $B(E2)\uparrow$ and $E2$

General features along with the details of the model has been well described elsewhere first[17] for $B(E2)\uparrow$ and secondly[19] for $E2$. Since our main interest here is to analyze the model predictions for identifying exotic

deformations, we simply highlight its basic equations and features. The principal equation of the model valid for both $B(E2)\uparrow$ and the corresponding excitation energy $E2$ is given by

$$\frac{C(N,Z)}{A} = \frac{1}{2}\Big[(1+\beta)\Big(\frac{\partial C}{\partial N}\Big)_Z + (1-\beta)\Big(\frac{\partial C}{\partial Z}\Big)_N\Big], \tag{1}$$

where N, Z and A refer to the neutron, proton and mass numbers of the given nucleus. β is the usual asymmetry parameter (N-Z)/A of the nucleus. The variable C represents both the physical quantities $B(E2)\uparrow$ and $E2$. As we can see, the relation (1) connects both $B(E2)\uparrow$ and $E2$ of a given nucleus to their partial derivatives with respect to the neutron and proton numbers N and Z. We may state here for sake of a comprehensive understanding, that the very basis behind its proposition goes to a similar equation being satisfied by the local energy component of the ground-state energy of a nucleus, specifically simulating its shell and deformation behavior in the infinite nuclear matter (INM) model [20, 21, 22, 23] of atomic nuclei primarily built on the basis of the generalized[24] HVH theorem[25] of many-body theory. Even though its proposition for these two physical quantities $B(E2)\uparrow$ and $E2$ has been made on close similarity with the local energy term of the INM model, it can be treated as a semi-empirical equation as it has been found[17, 19] to be satisfied by them by virtue of their slow variation with neutron and proton numbers N and Z locally. Hence the differential Eq. (1) for these two physical quantities may be better termed as localized semi-empirical equation like the difference equations of Ross and Bhaduri[15] and Pattnayak et al.[16]. we further like to highlight the interesting fact that the form of the differential equation (1) for these two physical quantities , for the local energy η of the INM model and the generalized HVH theorem concerning energy per nucleon of the asymmetric nuclear matter are all exactly similar in nature. Of course the genesis of the local energy relation in the INM model owes its origin to the generalized HVH theorem, whereas formulation of the differential equation for the two physical quantities $B(E2)\uparrow$ and $E2$ simulating the local energy η obviously got the same form. At the same time however we should note that while the HVH theorem is an exact theorem of the many-body theory, the differential equation (1) for all the physical quantities concerning the finite nucleus can be termed as model-dependent.

Then using the usual forward and backward definitions pair-wise for both the derivatives given by

$$\begin{aligned}
\Big(\partial C/\partial N\Big)_Z &\simeq \frac{1}{2}\Big[C[N+2,Z]-C[N,Z]\Big], \\
\Big(\partial C/\partial Z\Big)_N &\simeq \frac{1}{2}\Big[C[N,Z+2]-C[N,Z]\Big], \qquad (2)
\end{aligned}$$

and

$$\begin{aligned}
\Big(\partial C/\partial N\Big)_Z &\simeq \frac{1}{2}\Big[C[N,Z]-C[N-2,Z]\Big], \\
\Big(\partial C/\partial Z\Big)_N &\simeq \frac{1}{2}\Big[C[N,Z]-C[N,Z-2]\Big], \qquad (3)
\end{aligned}$$

the following two recursion relations in C would result

$$C[N,Z] = \frac{N}{A-2}C[N-2,Z] + \frac{Z}{A-2}C[N,Z-2], \quad (4)$$

$$C[N,Z] = \frac{N}{A+2}C[N+2,Z] + \frac{Z}{A+2}C[N,Z+2]. \quad (5)$$

These recursion relations connecting values of both $B(E2)\uparrow$ and $E2$ of the neighboring even-even nuclei from lower to higher mass and vice-verse, are primarily responsible in reaching out from known to the unknown terrain of the nuclear landscape, and thereby facilitate their predictions throughout. One may further note that the choice of either forward or backward definitions for both the two derivatives occurring in the Eq. (1) facilitate derivation of the close-knit first order recursion relations (4 and 5), each connecting three immediate neighboring even-even nuclei with neutron, proton and mass numbers differing at best by two units in the nucleon space as shown in Fig. 1(a), a fact which is of our primary concern. In contrast, mixed definitions, i.e, one forward and the backward for the derivatives would lead to second order relations connecting nuclei having mass numbers differing up to four units as can be seen in Fig. 1(b) and hence are ignored.

It is essential to stress here that these recursion relations not only connect isotopes of the same element but also different neighboring elements having proton numbers Z, Z-2 and Z+2. Therefore these recursion relations should not be interpreted as interpolation and extrapolation formulas. Moreover one should also note that since these relations connect isotopes of the neighboring elements, they facilitate prediction of the hitherto unknown data for the desired isotopes of a given element using the existing data of the relevant isotopes of the neighboring elements, even if its own data for the neighboring isotopes are either not available or scantly available. Even these interconnections connecting the isotopes of the neighboring elements provide possible means of bridging sharply changing isotopic variations of these two physical quantities across the isotopes of a given element.

In actual practice, we use the known available data in the neighborhood of a given nucleus in the two recursion relations (4) and (5) separately to generate its all possible values for $B(E2)\uparrow$ and $E2$. Since each of these relations can be rearranged in three different ways by shifting the three terms occurring in them from left to right and vice-verse, in principle one can generate up to six alternate values at best for a given nucleus. This is however subject to availability of the corresponding data. Again each of them being equally probable, the predicted value is then obtained by the arithmetic mean of all those generated values so obtained. We would like to comment here that this method of taking the arithmetic mean of the equally-probable generated values for a given isotope in a way, achieves some sort of uniqueness in the model predictions and at the same time automatically takes care of all possible local connections in a given locality. That is why this scheme has been found to be successful[17, 18, 19] in our limited predictions made earlier for both the physical quantities $B(E2)\uparrow$ and $E2$. Thus, our actual

calculation procedure uses the available experimental data in predicting values of these two physical quantities both for the known as well as for the hitherto unknown even-even nuclides. The predictions made in the first generation thus obtained for the unknown, are again used along with the known data in the second step to generate the next generation predictions and so on. This procedure is continued to reach out more and more neighboring regions of the nuclear chart. However we must mention here, that although this scheme in principle can be continued as widely as we please in the nuclear chart, in practice, it is terminated to avoid accumulation of errors. Nevertheless, we find that three to four generations are sufficient enough to reach out a large number of isotopes on either side of the normal β-stable valley for our present study.

3 Calculation of the Deformation Parameters from the $B(E2)\uparrow$ and $E2$ Model Predictions

Following the procedure laid down in the previous section, we have carried out the prediction scheme in the model using the combined data set of both Raman et al. [9] and Pritychenko et al. [11] near $N \sim Z \sim 28$ as the input experimental data. Accordingly the total number of $B(E2)\uparrow$ input data comprises altogether 330 even-even nuclides spread over the entire nuclear landscape ranging from O to Fm (Z=8 to 100), while the same for $E2$ is 557. Since our main interest in the present study is to identify possible occurrence of exotic regions of deformation in the n- and p-rich regions adjacent to the already known data valley, we have confined our calculations up to three to four generations of our prediction scheme. As a result, our present calculations have yielded hitherto unknown $B(E2)\uparrow$ data of 278 adjacent isotopes and $E2$ values of 175 isotopes apart from for those of the known data set.

In the next step, we used these predicted data for calculating the standard deformation parameters such as the quadrupole deformation β_2 and the ratio of β_2 to the Weisskopf single-particle $\beta_{2(sp)}$, termed here as β_r for simplicity. We would like to stress here that the value of the quadrupole deformation β_2 more or less reflects the nature of collectivity of a given nucleus. Its zero value would mean no deformation at all while its finite value would otherwise indicate increasing deformations or collectivity of a given nucleus. In general, its value up to 0.1 more or less reflects spherical nuclei while that of in the range 0.1-0.2 usually correspond to normal deformations. On the contrary its value in the range 0.3-0.5 has been shown[27, 28, 29, 30, 31] to reflect strong deformations in nuclei while its value of ≈0.55-0.65 has been considered[32, 33] to indicate super deformation. Therefore any such value beyond 0.3 for a given nucleus may be considered as to reflect large deformation. Apart from β_2, we

would also consider a supplementary quantity namely β_r as referred above . We may point out here that the ratio β_r has been considered[9] more significant in reflecting possible occurrence of the collective effects in nuclei.

The expressions for these quantities can be obtained in a model-dependent formalism, in which nuclei are treated as to have uniform charge distributions out to distance $R(\theta,\phi)$ and zero charge beyond. The defining equation for the quadrupole deformation parameter β_2 is as usual given by

$$R(\theta,\phi) = R_0[1+\beta_2 Y^*_{20}(\theta)], \tag{6}$$

where R_0 corresponds to the radius of a constant density undistorted nucleus and Y^*_{20} is the usual axially-symmetric spherical harmonics. Then the well-known relation that has been widely used in the literature[9] for computing the deformation parameter β_2 from the model-independent physical quantity $B(E2)\uparrow$ simply follows as [see for instance Roy & Nigam[34]]

$$\beta_2 = (4\pi/[3Zr_0^2A^{2/3}])[B(E2)\uparrow/e^2]^{1/2}. \tag{7}$$

Here r_0 is the usual nuclear radius parameter, the value of which is usually taken for compilation of such data as 1.2 fm and $B(E2)\uparrow$ is in units of e^2b^2. We would like to make a note here that the above expression for β_2 [notations may vary] has been widely used invariably by most of the groups see for instance Raman et al [9, 8] for extracting its value from the experimental $B(E2)\uparrow$ data.

For calculating the Weisskopf single-particle $\beta_{2(sp)}$ value, its expression can be derived by substituting the corresponding Weisskopf single-particle $B(E2)\uparrow$ value given by

$$B(E2)\uparrow_{sp} = 2.97\times10^{-5}A^{4/3}(e^2b^2) \tag{8}$$

in Eq. (7). Then the expression for $\beta_{2(sp)}$ simply follows as

$$\beta_{2(sp)} = (4\pi/[3Zr_0^2])\times\sqrt{0.297}, \tag{9}$$

which numerically can be simplified as 1.59/Z as has been done by Raman et al.[9]. Thus one can calculate the ratio β_r using Eqs. (7 and 9).

Apart from these two quantities, we also calculate another useful physical quantity, namely, the intrinsic electric quadrupole moment Q_0 in units of b given by

$$Q_0 = \left[\frac{16\pi}{5}\frac{B(E2)\uparrow}{e^2}\right]^{1/2}. \tag{10}$$

Thus we see that using these Eqs. (7, 9 and 10), all the relevant deformation parameters can be calculated from $B(E2)\uparrow$.

Before ending this section it is worth mentioning the fact that $\beta_{2(sp)}$ as can be seen from Eq. (9) remains a fractional constant for all the isotopes of a given element, and hence simply acts as a constant dividing factor for the quantity β_r for all those isotopes. Thus the numerical values of the deformation parameter β_r effectively gets enhanced for all those isotopes having large deformations by virtue of their larger β_2 values compared to those lying in the normal β-stable valley for a given element. As a result there cannot exist a definite value for this quantity to decide whether a particular isotope has a larger or a smaller deformation. Therefore the nature of deformation for a given isotope can only be ascertained by comparing its β_r value with those of its already known neighboring isotopes.

4 Results and Discussion

4.1 Identification of Exotic Deformed Nuclides

As per the details laid down above, we have first carried out the predictions of $E2$ and $B(E2)\uparrow$ data for the desired isotopes lying both in the known and the hitherto unknown regions of the nuclear chart. Then using these predicted data we subsequently calculated the deformation parameters β_2 and β_r by using the formulas (7,9). Our calculations have yielded $B(E2)\uparrow$ values of altogether 608 nuclides which include the input data of 330. Similarly our $E2$ predictions have yielded 732 nuclides that include input data of 557. Since our main interest being the identification of the possible exotic deformations in the hitherto unknown data regions, we present here in Table 1 only such data that are confined to those regions. We also present in the same table the calculated values of the deformation parameters β_2, β_r and Q_0.

In general, one can easily identify possible occurrence of the increasing collectivity and the consequent exotic deformations specially from the relatively larger values of β_2 and β_r from Table 1. As stated earlier any value of β_2 larger than 0.3 more or less reflects higher deformation and increasing collectivity of the given nucleus. Such observations can be further supplemented by the increasing values of β_r. However, for sake of conveying better visual display of such occurrences as scrutinized from the tabulated values, we graphically present values of these two deformation parameters for the isotope series as isolines only for those elements in the Figs. 2-7. Accordingly the graphs displayed in these figures correspond to such elements having proton number Z=10, 22, 24, 26, 28, 36, 38, 40, 42, 52, 54, 56, 58, 60, 62, 64, 66 and Z=92. We would like to again stress here that our choice of

these elements purely follows from our primary interest of identifying any possibility of exotic deformation in the exotic n- and p-rich regions of the nuclear chart. Consequently our close scrutiny of Table 1 shows increasing trends in the values of the deformation parameters for either in the n-rich or p-rich or both for the isotopes of the stated elements except however for Z=66 . For instance the β_2 value increases from 0.075 to 0.513 with increasing neutron number from N=32 to 38, while β_r values increase from 1.043 to 7.116 for the element Z=22. We have intentionally chosen to include the isoline for Z=66 just to highlight how such cases need not be considered due to the uninteresting nature of variation of the deformation parameters in the exotic n- and p-rich regions. For sake of comparative analysis and continuity in the graphical presentations, we have also included in these graphs our predictions in the known-data regions along with the adopted experimental values[9, 11] to help us to compare the relative values of both β_2 and β_r in our endeavor for identification of possible exotic deformations. Inclusion of the adopted experimental values in these graphs on the other hand would testify the goodness of the model predictions. In fact one can easily identify hitherto unknown-data isotopes from these graphs having large values of β_2 (≥ 0.3)and relatively larger values of β_r both in the n- and p-rich regions. Such relatively large values of these parameters obviously signify possible occurrence of exotic deformations for those isotopes.

Now coming to analyzing the individual cases, we find [see Figs. 2 (a) and Table 1] the values of the deformation parameter β_2 as 0.59 and 0.63 respectively at N=20 and 22 for Ne (Z=10). Despite N=20 being a magic number and N=22 is close to it, both these two n-rich isotopes are found to have such large values of β_2. On the other hand the β_r values of these isotopes are respectively 3.73 and 3.99, which are definitely larger than those of its own known neighbors as can be seen from Fig. 5 (a). Thus such increase is a clear indication of the possible occurrence of higher deformations in both ^{30}Ne and ^{32}Ne. Fortunately this finding of ours is well-supported by the recent experimental observation of enhanced collectivity for ^{30}Ne and the resulting disappearance of N=20 shell-closure by Yanagisawa et al.[6]. The authors of this experiment have attributed such occurrence of strong collectivity by breaking of the N=20 shell-closure by the intruder states from the pf-shell and hence are in favor of its inclusion in the "Island of Inversion" [35, 36]. Even the neighboring nuclide ^{34}Mg has been also found to be highly deformed as its β_2 value is 0.50 [see Table 1] in agreement with the experimental finding by Iwasaki et al. [37]. Incidentally this nuclide has also the same neutron number N=22 as that of ^{32}Ne.

Our close scrutiny [see Fig. 4 (a)] also lead us to find possible occurrence of large collectivity for ^{60}Ti as its β_2 value is 0.51, which is almost close to that of super deformation. Its β_r value has been found to be 7.11 which is again much larger compared to its neighboring known isotopes [see Fig. 7 (a)]. Accordingly this n-rich isotope of Ti is most likely be heavily deformed despite its neutron number 38 is very close to the semi-magic number 40 and

its proton number is also very close to the magic number 20, thereby clearly supporting the possible manifestation for the occurrence of another "Island of Inversion" caused by the intruder states from gd-shell[30].

Similarly such occurrences are also seen in case of $^{42,62,64}Cr$, $^{50,68}Fe$ and $^{52,72}Ni$ [see Figs. 2(b-d), 5(b-d) for β_2 and β_r respectively]. The β_2 values for all these nuclei lie in the range 0.29-0.41 signifying large collectivity. We also see that the β_r values for all these nuclei lying in the range 4.96-6.13 are well above the corresponding values of their neighboring known isotopes. Incidentally these predictions of ours are again well-supported by the recent experimental observation of increased quadrupole collectivity in ^{64}Cr and ^{68}Fe in a Coulomb-excitation experiment by Crawford et al. [7]. It is further interesting to find more support from another experimental observation of strong deformation by Sorlin et al [30] for the isotopes $^{60,62}Cr$. In all these n-rich isotopes including ^{60}Ti as stated above , the N=40 sub-shell closure most possibly gets broken due to the intruder orbitals $g_{9/2}$ and $d_{5/2}$ leading to strong collectivity in agreement with the conclusions arrived at by Sorlin et al. [30].

Concerning isotopes of Kr, Sr and Zr (Z=36, 38 and 40), we find the exotic isotopes $^{70,72,96}Kr$, $^{74,76}Sr$ and $^{78,80,106,108}Zr$ to have values of β_2 lying in the range 0.40-0.49 [see Figs. 2(e-f), 4(b)], while those of β_r lie in the range 10.3-11.6 [see Figs. 5(e-f), 7(b)]. Obviously such values of β_2 for these isotopes are quite large enough to signify high deformations in them. It is quite satisfying to note here that our present finding of large deformation with a β_2 value of 0.4 for ^{80}Zr in fact has been well-corroborated by Lister et al.[28] long back experimentally. One can also see that the n-rich isotope ^{102}Sr [see Figs. 4(b) and 7(b)] can also be treated as highly deformed as its β_2 and β_r values are almost close to the above ranges. For the neighboring element Mo, we also find relatively larger values of β_2 lying in the range 0.39-0.46 [see Fig. 3(a)] for the isotopes $^{82,84,110,112}Mo$. Whereas their β_r values lying in the range 10.3-12.2 are quite large enough compared to their known neighbors qualifying them to have large deformations [see Fig. 6(a)]. Prediction of such strong collectvity for the exotic isotopes ^{108}Zr and ^{112}Mo may be again connected to the possible existence of another "Island of Inversion" by breaking of the N=70 sub-shell closure by the intruder states from hfp- shell. Thus the existence of two "Islands of Inversion" already detected experimentally with the breaking of shell-closures at N=20 and N=40, and our present prediction of another one at N=70 sub-shell closure appears to be a general feature of nuclear dynamics in the exotic n-rich regions of the nuclear chart.

Similarly for the isotopes of Te, Xe and Ba (Z=52, 54 and 56), we see relatively higher than normal deformations for the nuclides ^{140}Te,^{144}Xe and ^{148}Ba as their β_2 values range from 0.25 to 0.33 [see Fig. 3(b-d)]. The same feature is well reflected with the wide-ranging values of β_r from 7.5 to 11.7 [see Fig. 6(b-d)]. We would like to further add here that our calculation also shows the p-rich isotope ^{122}Ba to be well-deformed [see Fig. 3(d) and

6(d)] in agreement with the experimental findings by Morikawa et al.[26].

Concerning the isotopes of Ce, Nd, Sm and Gd (Z=58, 60, 62 and 64), we find the values of β_2 to lie in the range 0.36-0.46 [see Figs. 3(e-f), 4(c-d)], thereby indicating possible occurrence of exotic deformations for the isotopes ^{122}Ce, $^{128,156}Nd$, $^{130,132,158,160}Sm$ and $^{138,162,164,166}Gd$. These findings are once again well supported by the values of β_r lying in the range 14.2-17.5 [see Figs. 6(e-f), 7(c-d)]. As usual these values are larger than the corresponding values of their respective known neighboring isotopes.

As mentioned earlier, we have also shown β_2 and β_r isolines for Z=66 in the Figs. 4 (e) and 7 (e) just to highlight the border cases that we have ignored. We see that both the deformation parameters almost remain unchanged with increase of neutrons and even show decreasing trends. This is perhaps a clear indication of no substantive change in nuclear structure. Hence such variation in the deformation parameters for the isolines of other elements that we have not included in our present study may not be of much interest.

Finally coming to the case of Uranium (Z=92) in the very heavy-mass region as shown in the Figs. 4 (f) and 7 (f) , we find slight increasing trends in the values of the deformation parameters with the increasing neutron number from N=146 to 154. We see that β_2 value increases monotonically from 0.29 to 0.30 and those of β_r from 16.73 to 18.62. Therefore we are of the view that the tendency for higher deformation possibly exists, but without having any dramatic change in the nuclear structure.

Thus, in general the regions in the nuclear chart corresponding to the said isotopes discussed above as well as some in the immediate neighborhood could be possible regions of large scale exotic deformations, as the values of the quadrupole deformation parameter β_2 are closer to and even greater than 0.3. As usual the values of β_r are are relatively larger than their respective known neighboring isotopes. Expectedly such behavior is well supported by the values of the other physical quantity namely the intrinsic electric quadrupole moment Q_0, which we have plotted for all the isotope series against the neutron number N in Figs. 8-10. The increasing value of Q_0 for those isotopes as seen from these figures clearly corroborate our findings.

Even more importantly, all these findings of exotic deformation listed above have been well borne out with our predicted values of the other physical quantity, namely, the excitation energy $E2$ as can be seen from Table 1. Graphical presentations as shown in Figs. 11-13 also bear out the same features more convincingly. We should remember that unlike the deformation parameters derived from the values of $B(E2)\uparrow$, values of $E2$ are determined completely independent of the former. Hence the nature of the isotopic behavior of $E2$ is expected not only independent but at the same time opposite to that of the $B(E2)\uparrow$. This is exactly the case as it should be with $E2$, as we see from the complementary nature of the graphs displayed in the Figs. 11-13 in contrast to

those of the deformation parameters β_2 and β_r . We find that the $E2$ values of the concerned isotopes claimed to have large deformations are almost increasingly small as they lie on the peripheral portions of the graphs, in contrast to the opposite behavior in case of $B(E2)\uparrow$ and the deformation parameters derived from it such as β_2 , β_r and Q_0. Numerically our predicted E2 values for almost all the isotopes of Ne, Ti, Cr, Fe, Ni and Kr in the low- and medium-mass regions claimed to have large deformations lie in the range 0.35-1.4 MeV. Even experimental E2 values of some of these isotopes also lie in the range 0.7- 1.1 MeV [see for instance Fig. 11 for the isotopes ^{50}Fe, ^{72}Kr and ^{72}Ni]. Whereas both predicted and experimental E2 values of the claimed isotopes having high deformations in the heavy-mass region almost lie in the range 0.07-0.5 MeV. Thus our predicted E2 values convincingly support possible existence of exotic high deformations perceived from the predicted $B(E2)\uparrow$ values and the deformation parameters calculated from it.

Before ending this section, we just want to highlight here regarding the nature of agreement of our model predictions with the adopted $B(E2)$ and E2 data, which of course has been well-demonstrated while developing[17, 19] the model. Here the goodness of agreement is once again borne out from the close agreement of the derived quantities β_2, β_r and Q_0, and $E2$ itself as seen from the Figs. 2-13. It is rather remarkable to see the nature of good agreement of the sharply changing isotopic variations of our model predictions with those of experiment in almost all the cases as seen from the Figs. 2-13, vindicating our assertion made earlier about the recursion relations (4 and 5) that they should not be treated as interpolation or extrapolation formulas. The data of the isotopes of the neighboring elements play decisive role in this regard as the recursion relations connect nuclei having proton numbers Z, Z-2 and Z+2. Thus such remarkable agreement with the experimental data [9, 11] throughout and particularly the nature of sharply changing isotopic variations in most cases bear clear testimony of the goodness of the GDE model.

4.2 Comparison with the Latest Experimental Data

Having identified possible regions of exotic deformation with our predicted data, it would be of interest to compare our predicted values of $E2$ and $B(E2)\uparrow$ against any new experimental data if available, which we have not included in our prediction scheme. This would be highly desirable as they would provide the test of reliability of our predictions and establish our model for good. In this connection, we happened to come across a recent arxive article by Pritychenko et al. [38] of their latest data compilation for some of the neighboring nuclides adjacent to the already known data set. Obviously this new adopted data set at least would give us a good opportunity to test our model predictions for some if not for all. From our close scrutiny of our predicted data given in Table

1 and those of the latest experimental data [38], we find that hitherto unknown data of 77 nuclides in case of $B(E2)\uparrow$ and 65 nuclides in case of of $E2$ are available for this comparative analysis. With this view we followed Raman et al's [9] prescription of comparing in terms of the order of agreement of our predicted data with these new experimental data. Accordingly we have presented the ratio of the predicted values with those of the newly adopted data for $E2$ and $B(E2)\uparrow$ respectively in Figs. 14 and 15. One can easily see that 60 out of 65 data points for $E2$ (see Fig. 14) lie within the box indicating the percentage of agreement as 92%. Such an agreement can be termed excellent as per the yardstick stipulated by Raman et al [9].

Similarly in case of $B(E2)\uparrow$ predictions, we see that 62 data points out of 77 lie within the box (see Fig. 15) with the resulting percentage of agreement as 81% . Compared to $E2$ the degree of agreement for $B(E2)\uparrow$ is somewhat less. However on close scrutiny we find, that most of the 14 cases that lie outside the box (see Fig. 15) have relatively larger experimental uncertainty[38] to the tune of 40 to 109%. Just to cite few examples , the adopted $B(E2)\uparrow$ value of ^{148}Gd is 0.2279 $(^{+.1144}_{-.0548})$, while the same for ^{124}Cd is 0.35$\pm$.19 and that of ^{74}Ni is 0.0642$\pm$.0442. All these values quoted here are in the usual units of e^2b^2. Thus such large experimental uncertainty would obviously affect the actual experimental value. Secondly for some of these 14 cases, the adopted $B(E2)\uparrow$ values are themselves negligibly small, and accordingly any good agreement in such cases may not be feasible to achieve. Just to cite few such examples for which the adopted $B(E2)\uparrow$ values being very small are 0.0096$\pm$.0030, 0.00373$\pm$.00038 and 0.060$\pm$.020 in case of ^{24}Si, ^{50}Ca, and ^{56}Ti respectively. In view of these two aspects we can very well say, that the quality of agreement of our model predictions for $B(E2)\uparrow$ with the newly adopted data is rather excellent. Thus, more or less we see that our predictions made in our GDE model both for $E2$ and $B(E2)\uparrow$ very well stand the test of reliability and thereby support once again the goodness of the GDE model.

5 Concluding Remarks

In conclusion, we would like to say that our main concern in the present work is to identify possible occurrence of large deformations for some of the even-even nuclides lying in the n- and p-rich regions of the nuclear chart from our extensive predictions for the reduced quadrupole transition probability $B(E2)\uparrow$ and the complementary excitation energy $E2$. We have made these predictions using our recently developed Generalized Differential Equation model for these two physical quantities. These predictions include the hitherto unknown data for the nuclides lying adjacent to the already known data-regions of Raman et al. [9] for most of the even-even isotopes

of Oxygen to Fermium (Z=8 to 100). For sake of facilitating our desired task, we have also included in our calculation values of the model-dependent deformation parameters such as β_2, the ratio of β_2 to the Weisskopf single-particle $\beta_{2(sp)}$ and and the intrinsic electric quadrupole moment Q_0 using the predicted values of $B(E2)\uparrow$ and $E2$. In this regard, our critical analysis of the resulting data convincingly support possible existence of large collectivity and the consequent exotic deformations for the nuclides $^{30,32}Ne$, ^{34}Mg, ^{60}Ti, $^{42,62,64}Cr$, $^{50,68}Fe$, $^{52,72}Ni$, $^{72,70,96}Kr$, $^{74,76}Sr$, $^{78,80,106,108}Zr$, $^{82,84,110,112}Mo$, ^{140}Te, ^{144}Xe, ^{148}Ba, ^{122}Ce, $^{128,156}Nd$, $^{130,132,158,160}Sm$ and $^{138,162,164,166}Gd$. The quadrupole deformation parameter β_2 for all these nuclei mostly exceeds 0.3 and even lies in the range 0.45-0.55 for some of them like $^{30,32}Ne$, ^{34}Mg, ^{60}Ti, ^{62}Cr, $^{72,70,96}Kr$, $^{74,76}Sr$, $^{106,108}Zr$ and ^{82}Mo. Such large collectivity is well supported by the corresponding relatively smaller values of the supplementary physical quantity, namely, the excitation energy E2. The E2 values mostly lie in the range 0.35-1.4 MeV for these nuclei in the low- and medium-mass region, while the same in heavy-mass region lie in the range 0.07-0.5 MeV. Even some of the available experimental data in this regard do lie in the range 0.7-1.1 MeV.

Our prediction of strong deformation in case of $^{30,32}Ne$ and ^{34}Mg in fact are in close agreement with the experimental observation by Yanagisawa et al.[6] and Iwasaki et al. [37] respectively leading to the existence of the ”Island of Inversion” caused by breaking of the N=20 shell-closure by the intruder states from the pf-shell[35, 36]. Similar predictions in case of ^{60}Ti, $^{62,64}Cr$, ^{68}Fe also agree with the experimental findings[7, 30] again leading to the existence of another ”Island of Inversion” caused by the breaking of the N=40 sub-shell closure by the intruder states from the gd-shell. Thus such agreement with the experimental findings in the medium-low and medium mass nuclei in the exotic n-rich regions have made us to conjecture the existence of another ”island of Inversion” in the heavy-mass region possibly caused by breaking of the N=70 sub-shell closure by the intruder states from the hfp-shell as we find strong deformation for the nuclides ^{108}Zr and ^{112}Mo. Thus it appears that the existence of such ”Islands of Inversion” in the exotic n-rich regions of the nuclear chart may be a general feature of nuclear dynamics waiting for to be explored by future experiments. In fact analysis[23] of two two-neutron separation energy systematics derived from mass predictions in the INM model of atomic nuclei supports the existence of such islands in the heavy-mass n-rich region of the nuclear chart apart from the ones in the lower- and medium-mass regions.

Apart from serving the primary purpose of the present work in predicting exotic deformations in the exotic regions of the nuclear chart as highlighted above, we also observe rather good agreement of our predictions with the adopted experimental data. Even our model could reproduce the sharply changing isotopic variations of the two physical quantities $B(E2)\uparrow$ and E2 in agreement with those of experiment, vindicating our assertion that the

recursion relations (4 , 5) derived in the model should not be treated as interpolation or extrapolation formulas. In this regard the interconnecting relations connecting the neighboring elements having proton number Z, Z-2 and Z+2 facilitate achieving this. This supplements our earlier observation of good agreement with experiment while developing[17, 19] the model.

Even to our satisfaction, we could further succeed in establishing the goodness of the model in comparing some of our predictions with the latest experimental data [38] which we have not included in our prediction process. In this respect it is quite remarkable to find, that the quality of agreement of our predictions for both these two physical quantities $B(E2)\uparrow$ and $E2$ is rather excellent.

ACKNOWLEDGMENTS

One of us (RCN) acknowledges some useful discussion with R. Sahu of the Department of Physics (BU) regarding the range of possible values of the quadrupole deformation parameter for relevant deformations in nuclei.

References

[1] N. Fukunishi, T. Otsuka and T. Sebe, Phys. Lett. **B96** (1992)279.

[2] F.K. Thielemann, K. L. Kratz, B. Pfeiffer, T. Rauscher, L. Van Wormer and M.C. Weischer, Nucl. Phys. **A570** (1994)329c

[3] C. Thibault *et al.*, Phys. Rev. **C 12** (1975)644

[4] O.B. Tarasov *et al.*, Phys. Rev. Lett. **102**(2009) 142501, Science Daily Feb.3 (2011).

[5] S. M. Lenz *et al.*, Phys. Rev. **C 82**(2010)054301

[6] Y.Yanagisawa *et al.*, Phys. Rev. Lett. **B 566**(2013)84

[7] H.L. Crawford, R.M. Clark, P. Fallon et al., Phys. Rev. Lett. **110** (2013) 242701

[8] S. Raman, C. W. Nestor, K. H. Bhatt, Phys. Rev. **C 37**(1988) 805

[9] S. Raman, C. W. Nestor, Jr, P. Tikkanen, At. Data and Nucl. Data Tables 78(2001)1-128

[10] S. Raman, C. H. Malarey, W. T. Milner, C. W. Nestor, Jr., and P. H. Stelson, At. Data and Nucl. Data Tables **36** (1987)1-96

[11] B. Pritychenko, J. Choquette, M. Horoi, B. Karamy and B. Singh , At. Data and Nucl. Data Tables 98(2012)798-811

[12] L. Grodzins, Phys. Lett. **2**(1962) 88

[13] A. Bohr and B. R. Mottelson, Mat. Fys. Medd. Dan. Vid. Selsk. **27**(1953) No. 16

[14] C. W. Wang, G. C. Kiang, L. I. Kiang, C. C. Hsu, and E. K. Lin, Chinese Int. J. Phys. **18** (1980) 151

[15] C. K. Ross and R. K. Bhaduri, Nucl. Phys. **A 196** (1972)369

[16] R. Patnaik, R. Patra and L. Satpathy, Phys. Rev.**C12** (1975) 2038

[17] S. Pattnaik and R. C. Nayak, Int. Jou. of Mod. Phys. **E23** (2014) 1450022

[18] R. C. Nayak and S. Pattnaik, Int. Jou. of Mod. Phys. **E24** (2015) 1550011

[19] R. C. Nayak and S. Pattnaik, Phys. Rev. **C 90** (2014) 057301

[20] L. Satpathy, J.Phys.**G13**(1987) 761

[21] R. C. Nayak and L. Satpathy, Atom. Data and Nucl. data Tables **73** (1999)213

[22] L. Satpathy, V. S. Uma Maheswari and R.C. Nayak, Phys. Rep. **319** (1999) 85

[23] R. C. Nayak and L. Satpathy, Atom. Data and Nucl. Data Tables **98** (2012)616

[24] L. Satpathy and R.C. Nayak, Phys. Rev. Lett. **51** (1983)1243

[25] N. H. Hugenholtz and L. Van Hove, Physica **24** (1958) 363.

[26] T. Morikawa et al., Phys. Rev. **C 46** (1992)R6

[27] C. J. Lister *et al.*, Phys. Rev. Lett. **49** (1982)308

[28] C. J. Lister *et al.*, Phys. Rev. Lett. **59** (1987)1270

[29] K. Heyde, J. Moreau and M. Waroquier, Phys. Rev. **C 29** (1984)1859

[30] O.Sorlin et al., Euro. Phys. Journ. **A 16** (2003)55

[31] W. Nazarewicz, Nucl. Phys. **A 435** (1985)397

[32] P. fallan, Nucl. Phys. **A 752** (2005)231c

[33] F. lerma et al., Phys. Rev. **C 67** (2003)044310

[34] R.R. Roy and B. P. Nigam, Nuclear Physicsi: Theory and Experiment, New Age International (P) Ltd. Publ. (1996), Page 273-275 [Original Publ.: John Wiley & Sons, Inc. New York, 1967]

[35] E. K. Warburton, J. A. Becker, B. A. Brown, Phys. Rev. **C 41** (1990)1147

[36] X. Campi et. al., Nucl. Phys. **A 251** (1975)193

[37] H. Iwasaki et al., Phys. Lett. **B 522**(2001)227

[38] B. Pritychenko, M. Birch, B. Singh, M. Horoi , ArXive 1312.5975v5(nucl-th)2014

~

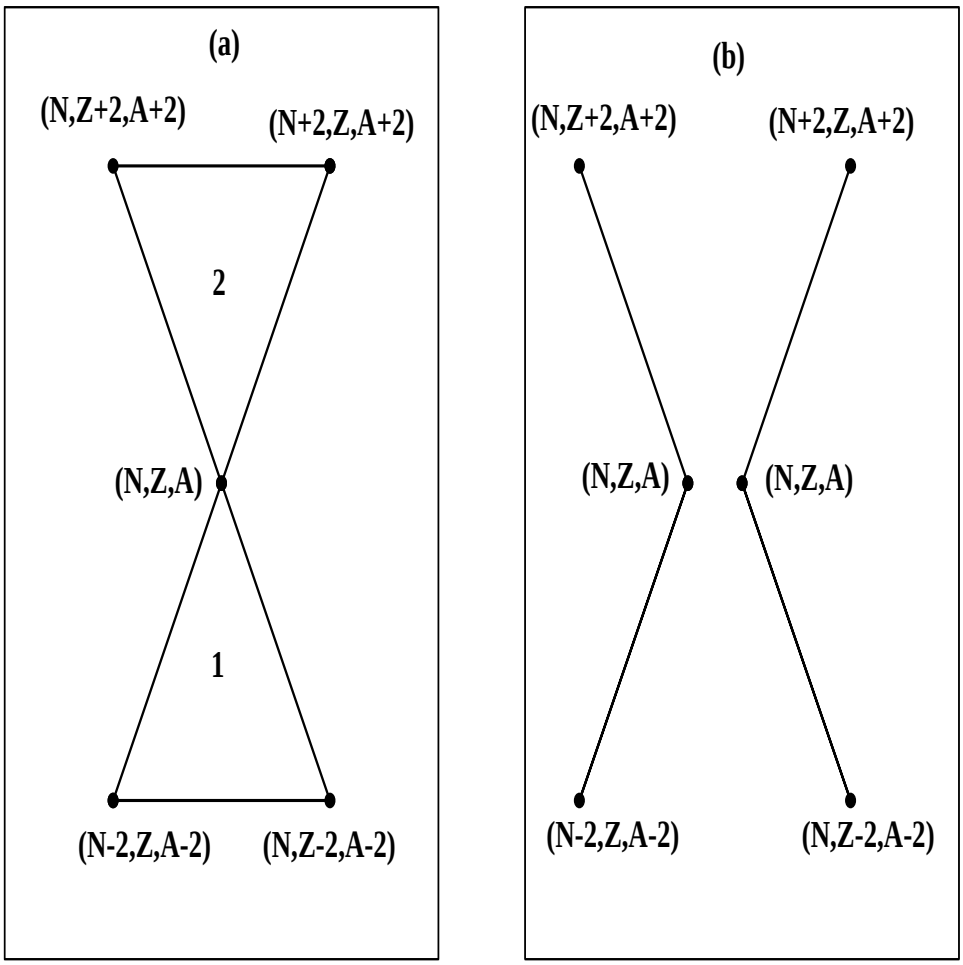

Figure 1: Schematic diagram showing how the recursion relations connect the neighboring even-even nuclei. (a) corresponds to the first order relations (4,5) connecting nuclei shown here as the vertices of the two triangles 1 and 2, while (b) shows those of the second order relations (see text for details).

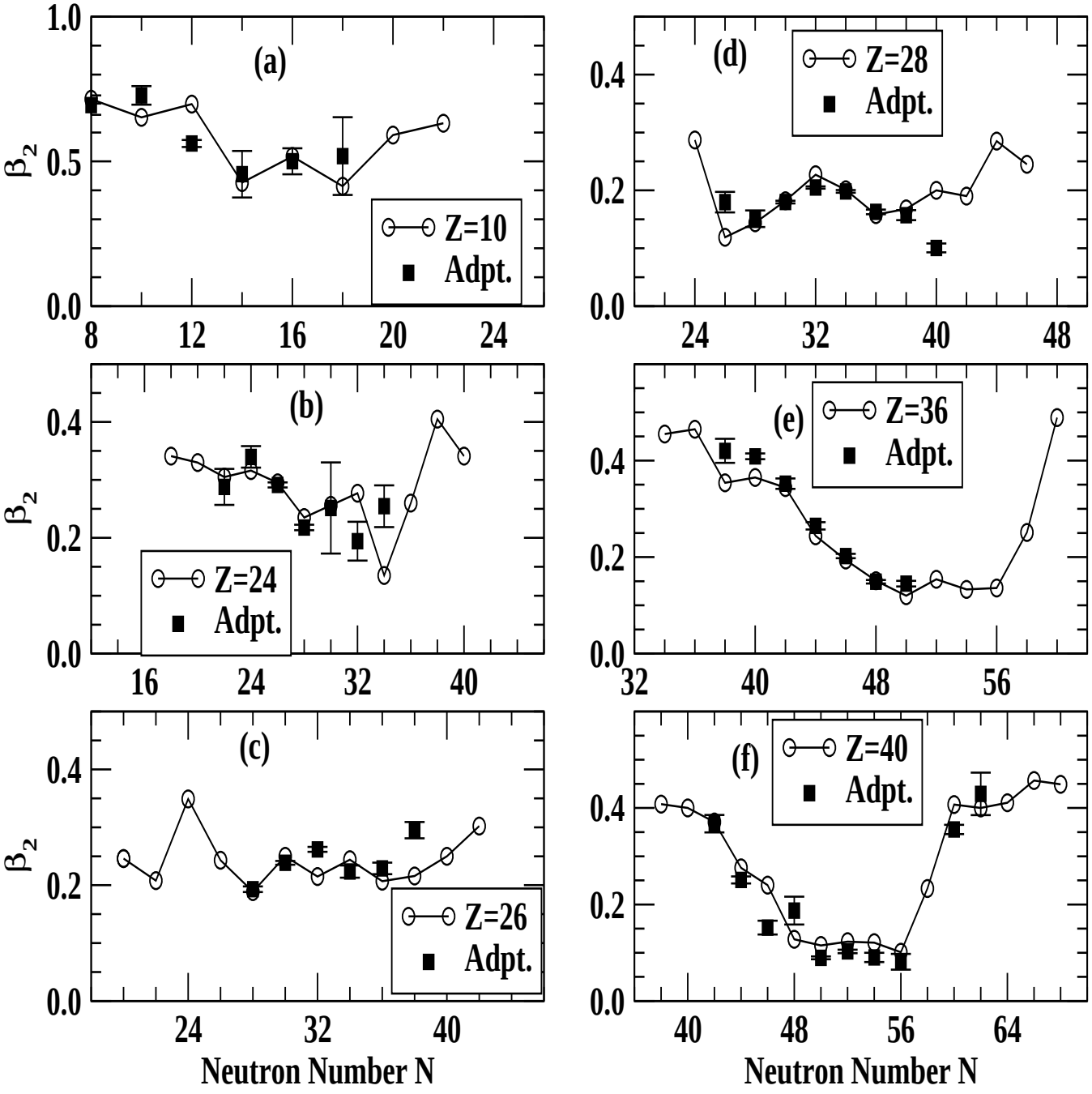

Figure 2: Values of the calculated quadrupole deformation parameter β_2 (see text) for the isotope series Z= 10, 24, 26, 28, 36 and 40 plotted here as isolines against neutron number N. Thick lines connecting open circles represent our predicted values while solid squares with vertical lines marked as [Adpt.] correspond to those of the adopted values[9, 11]. The vertical lines as usual represent the uncertainty in the adopted values.

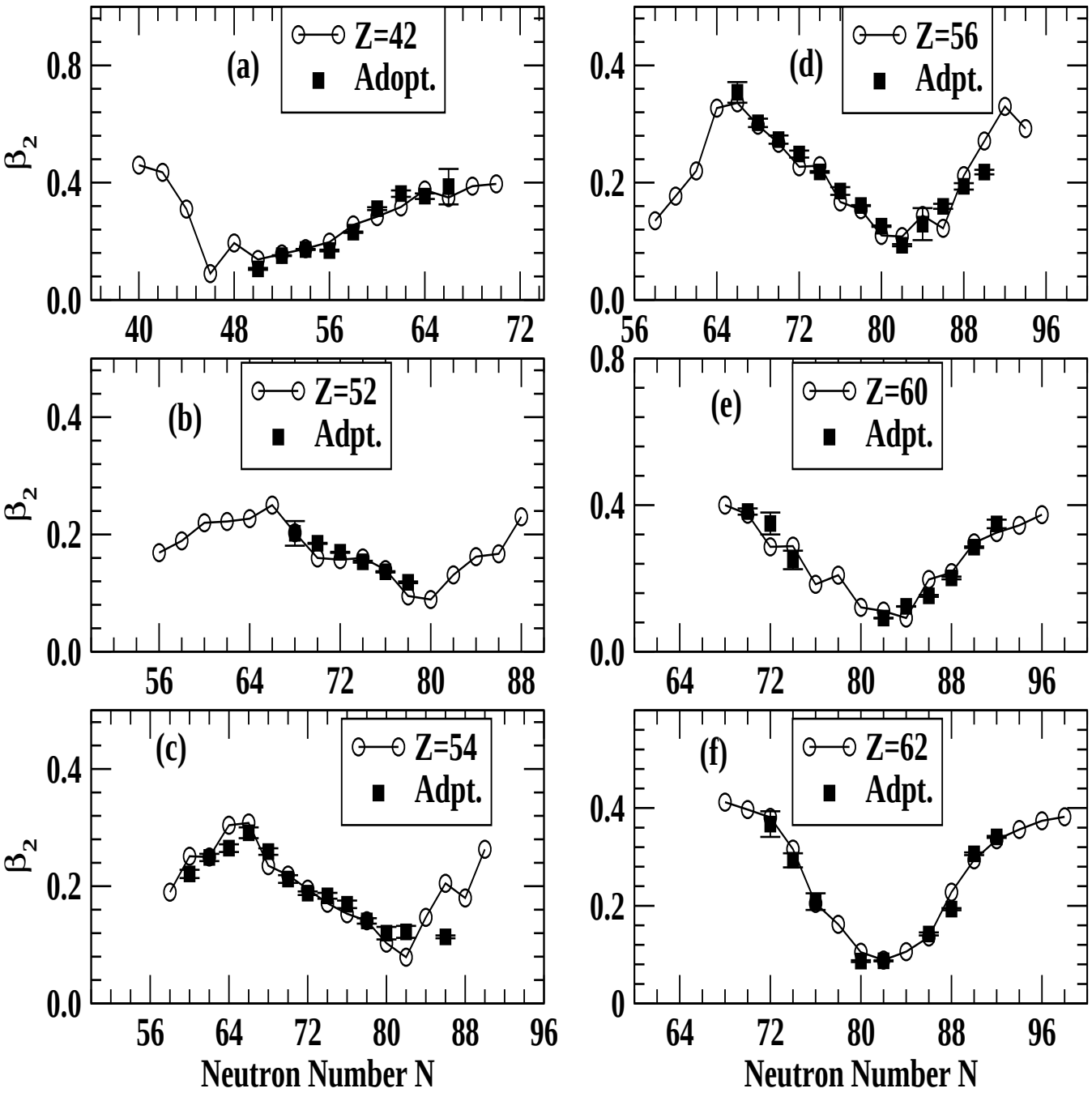

Figure 3: Same as Fig. 2 but for Z=42, 52, 54, 56, 60 and 62.

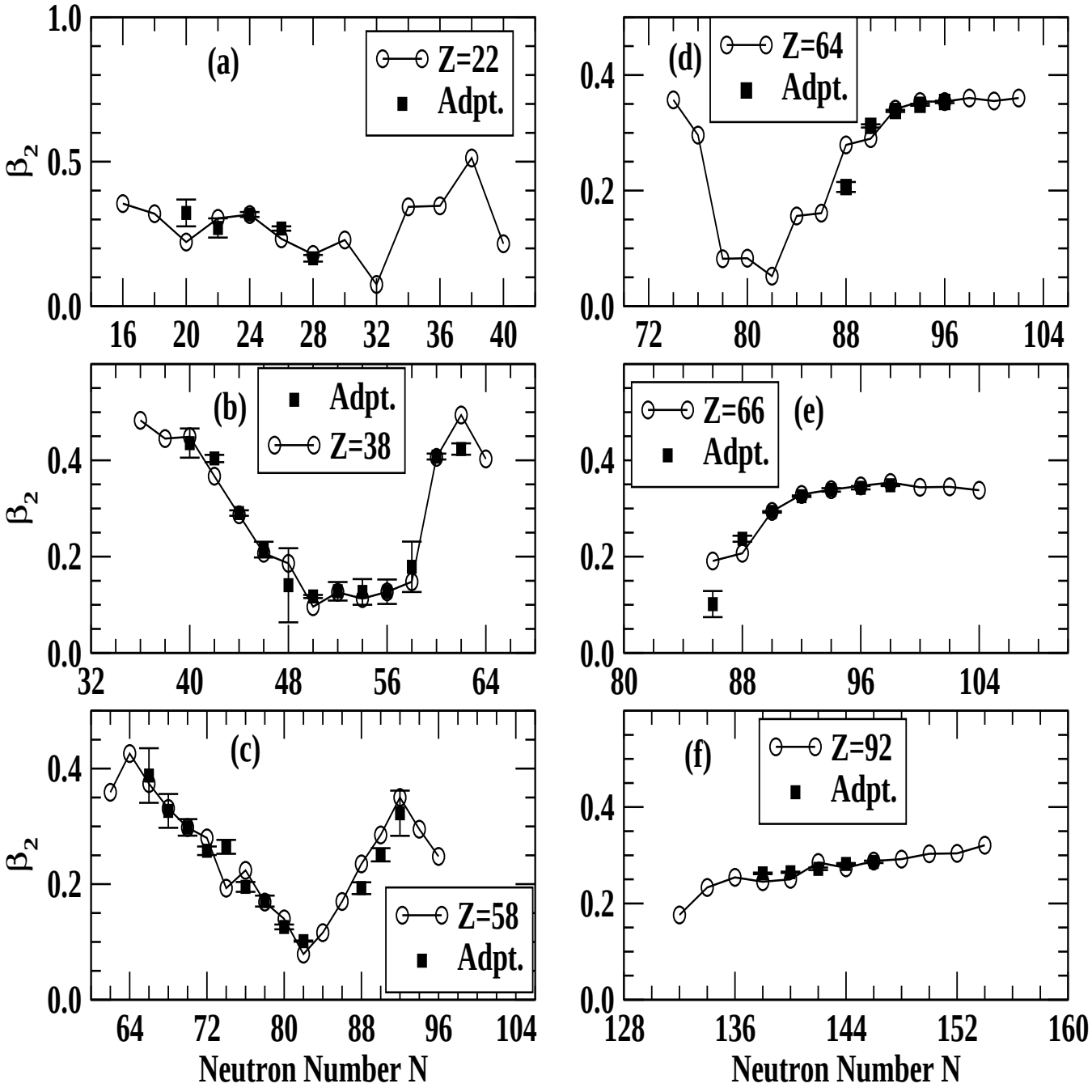

Figure 4: Same as Fig. 2 but for Z=22, 38, 58, 64, 66 and 92.

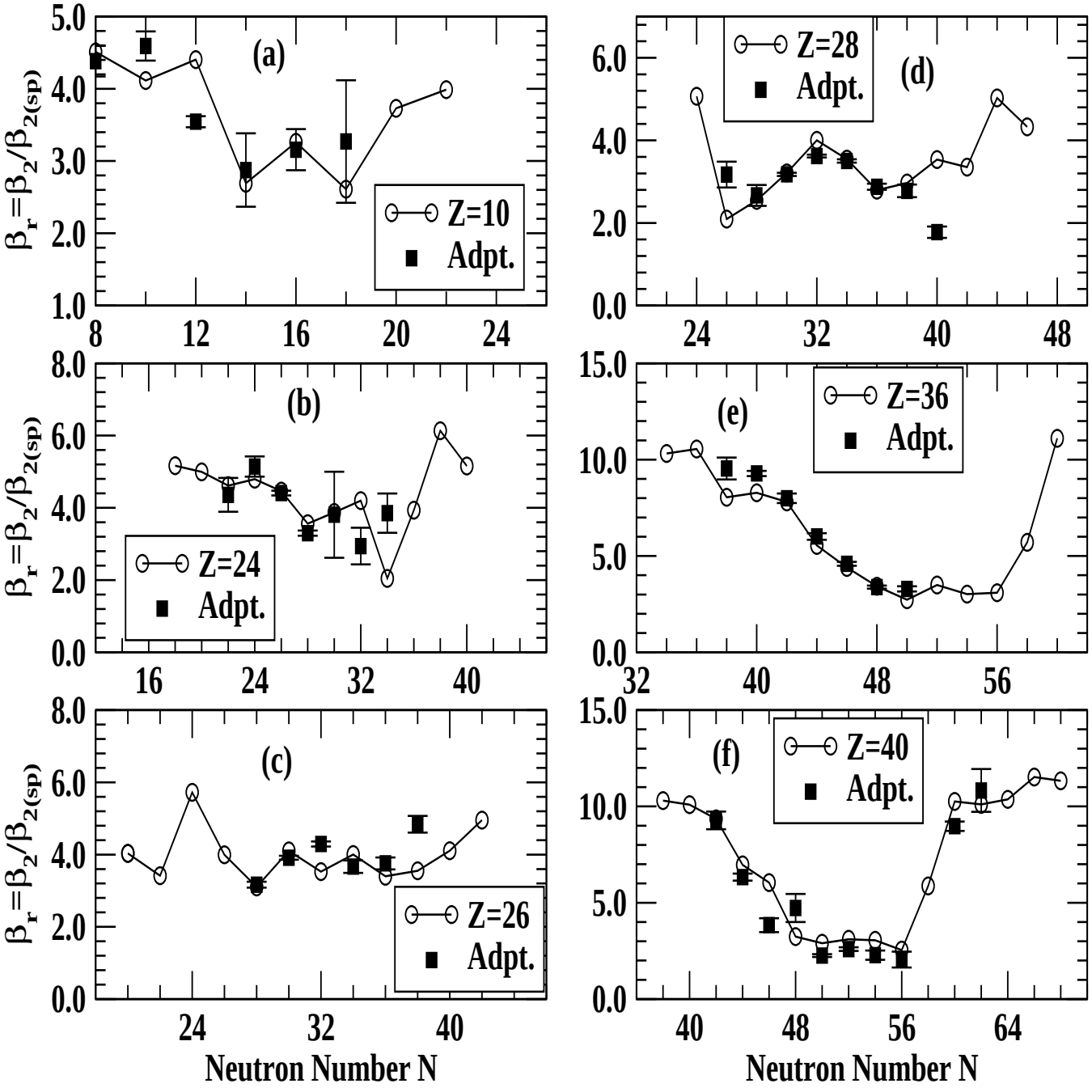

Figure 5: Similar to Fig. 2 but for the values of the deformation parameter β_r (see text) for the series Z=10,24, 26, 28,36 and 40.

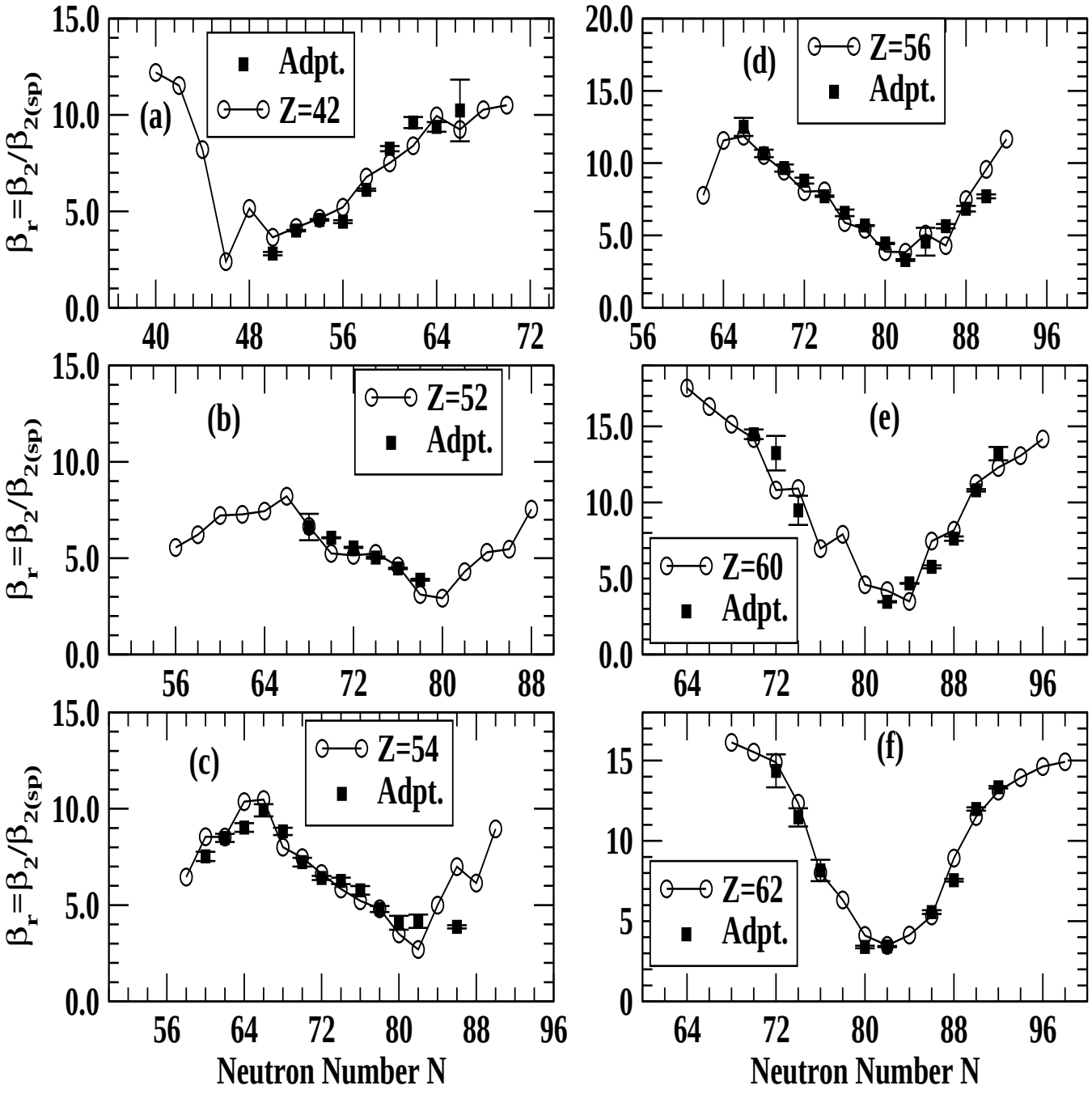

Figure 6: Similar to Fig. 3 but for the values of the deformation parameter β_r for Z=42, 52, 54, 56, 60 and 62.

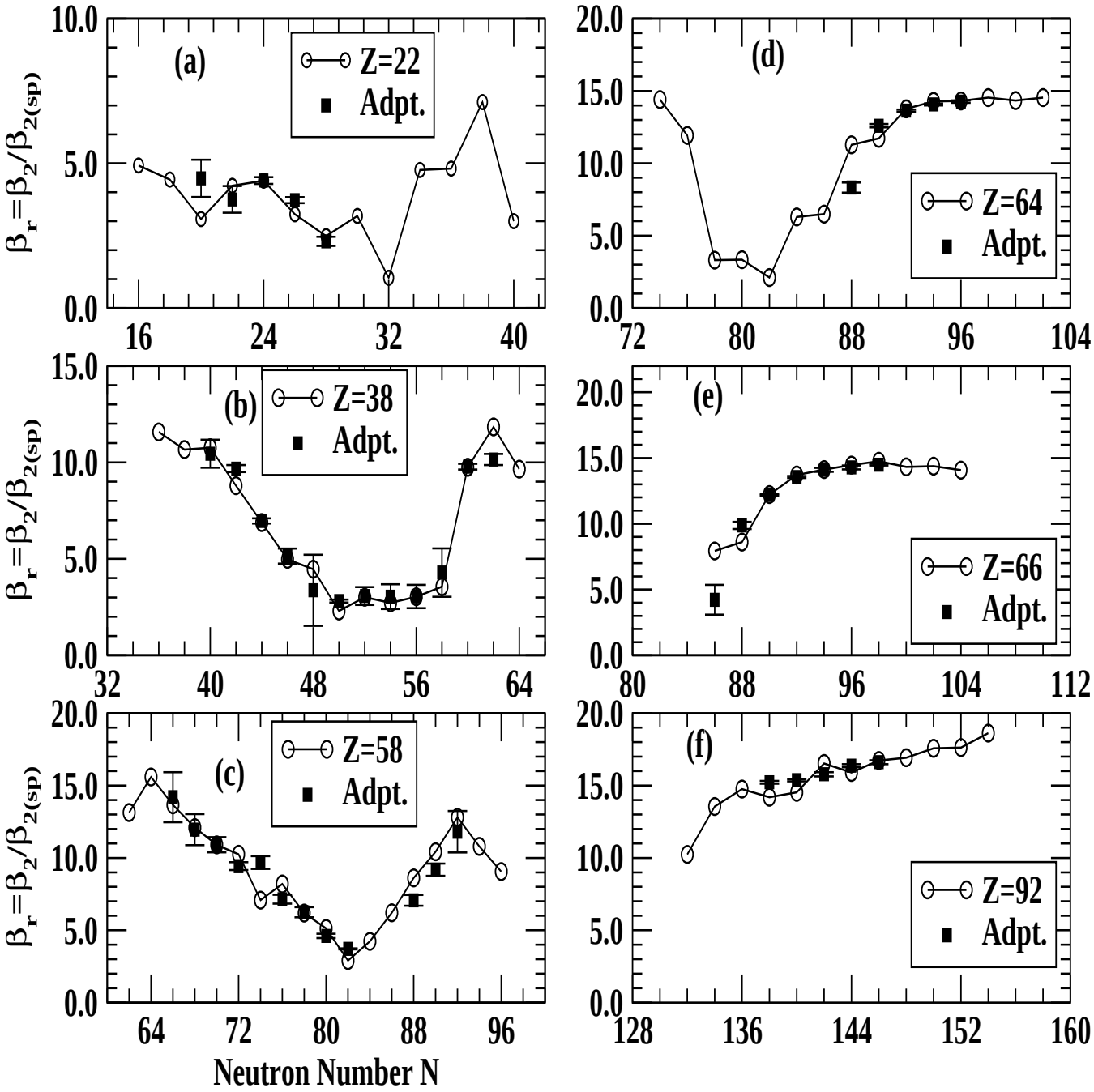

Figure 7: Similar to Fig. 4 but for the values of the deformation parameter β_r for Z=22, 38, 58, 64, 66 and 92.

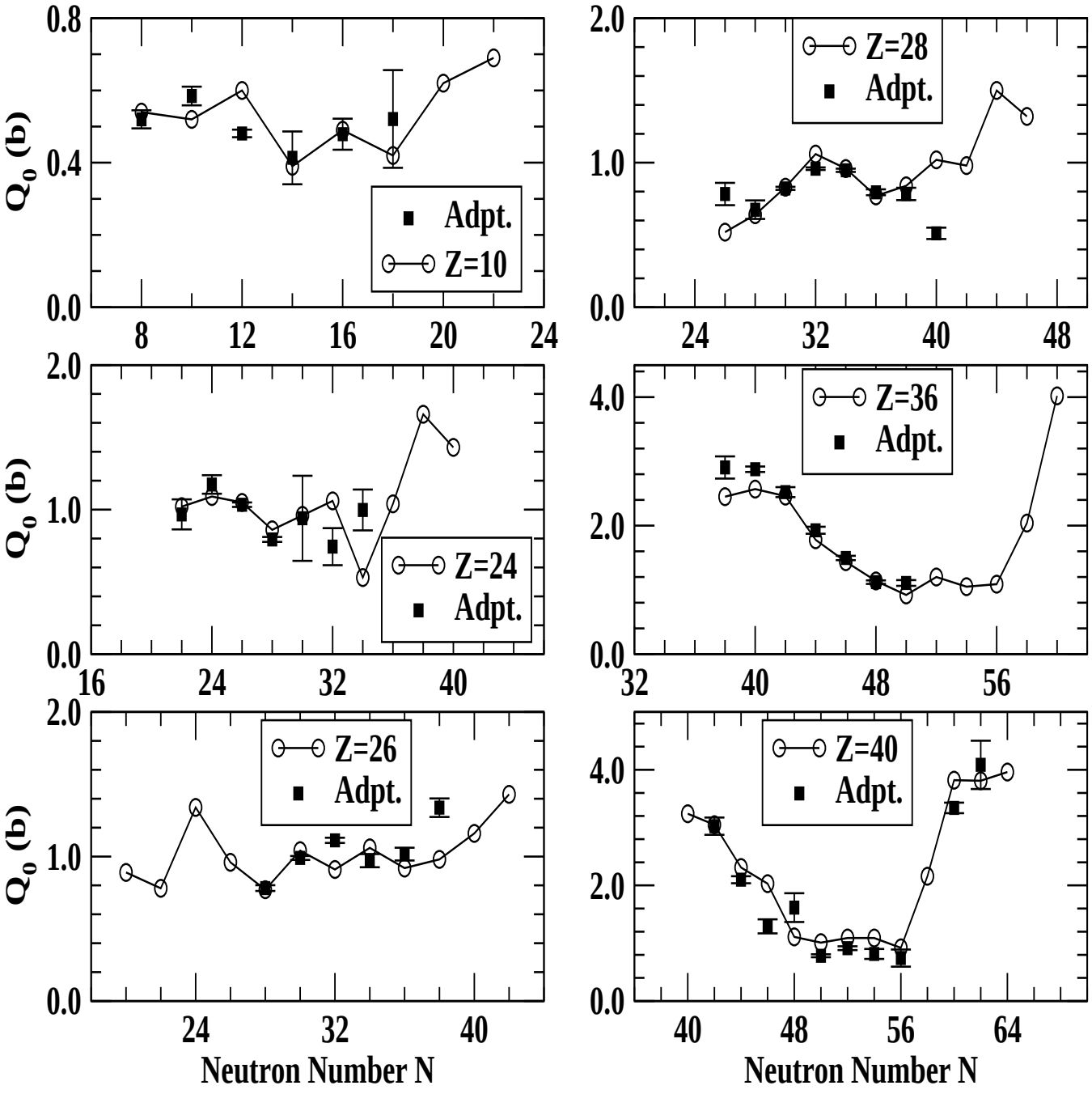

Figure 8: Similar to Figs. 2 but for the values of the Intrinsic Electric Quadrupole Moment Q_0 for the series Z=10, 24, 26, 28, 36 and 40

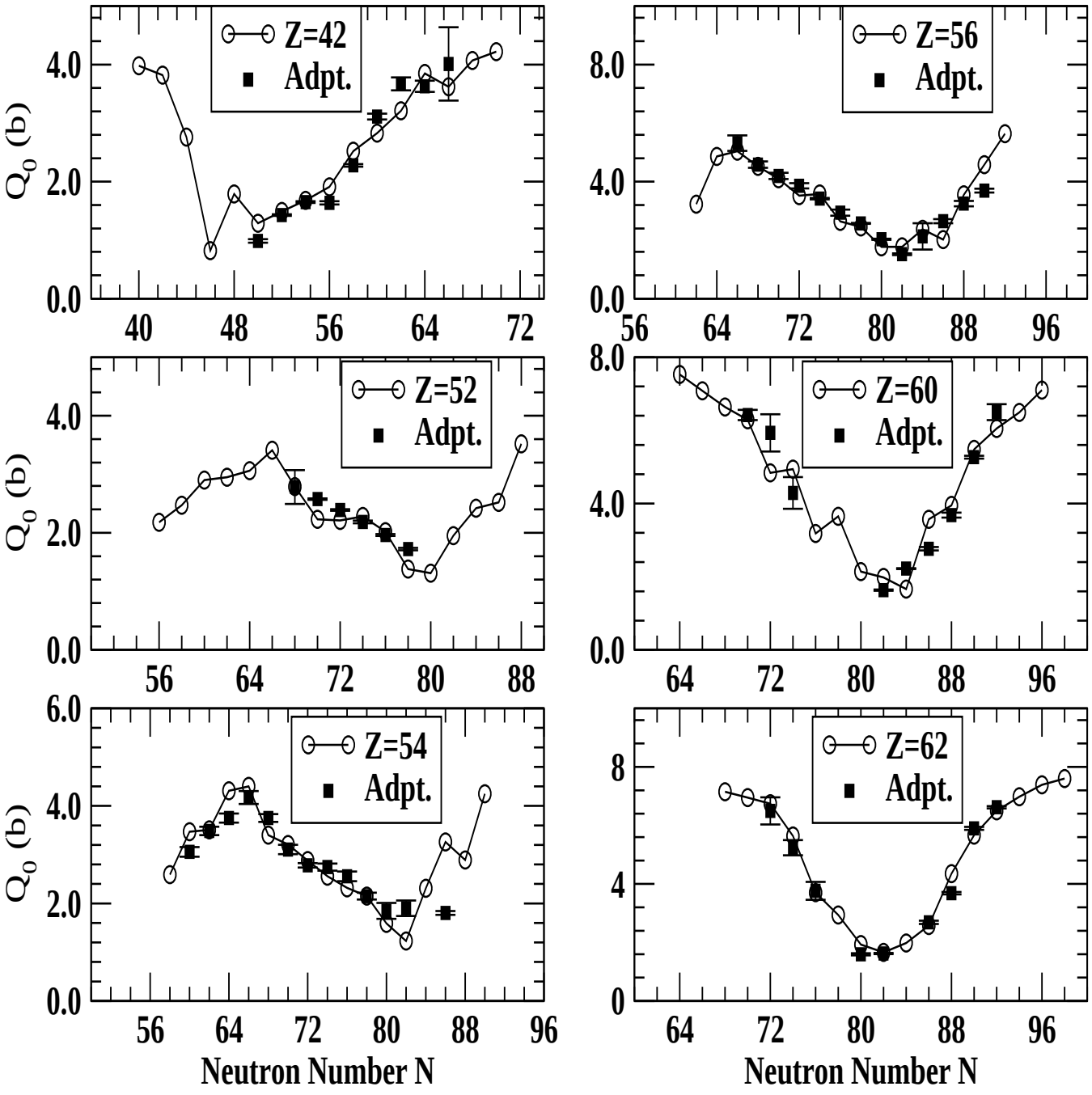

Figure 9: Similar to Figs. 3 but for the values of the Intrinsic Electric Quadrupole Moment Q_0 for the series Z=42, 52, 54,56,60 and 62

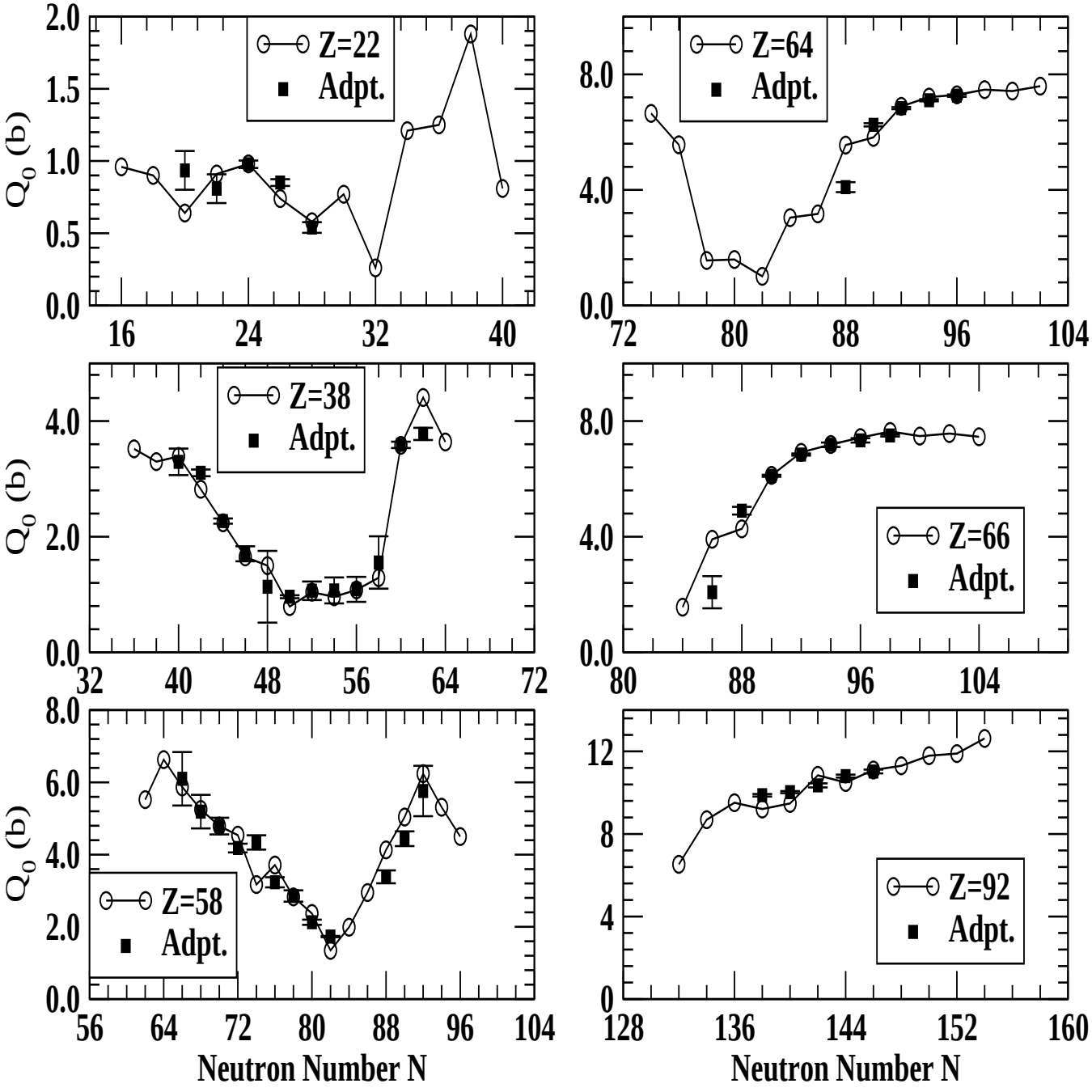

Figure 10: Similar to Figs. 4 but for the values of the Intrinsic Electric Quadrupole Moment Q_0 for the series Z= 22, 38, 58, 64, 66 and 92.

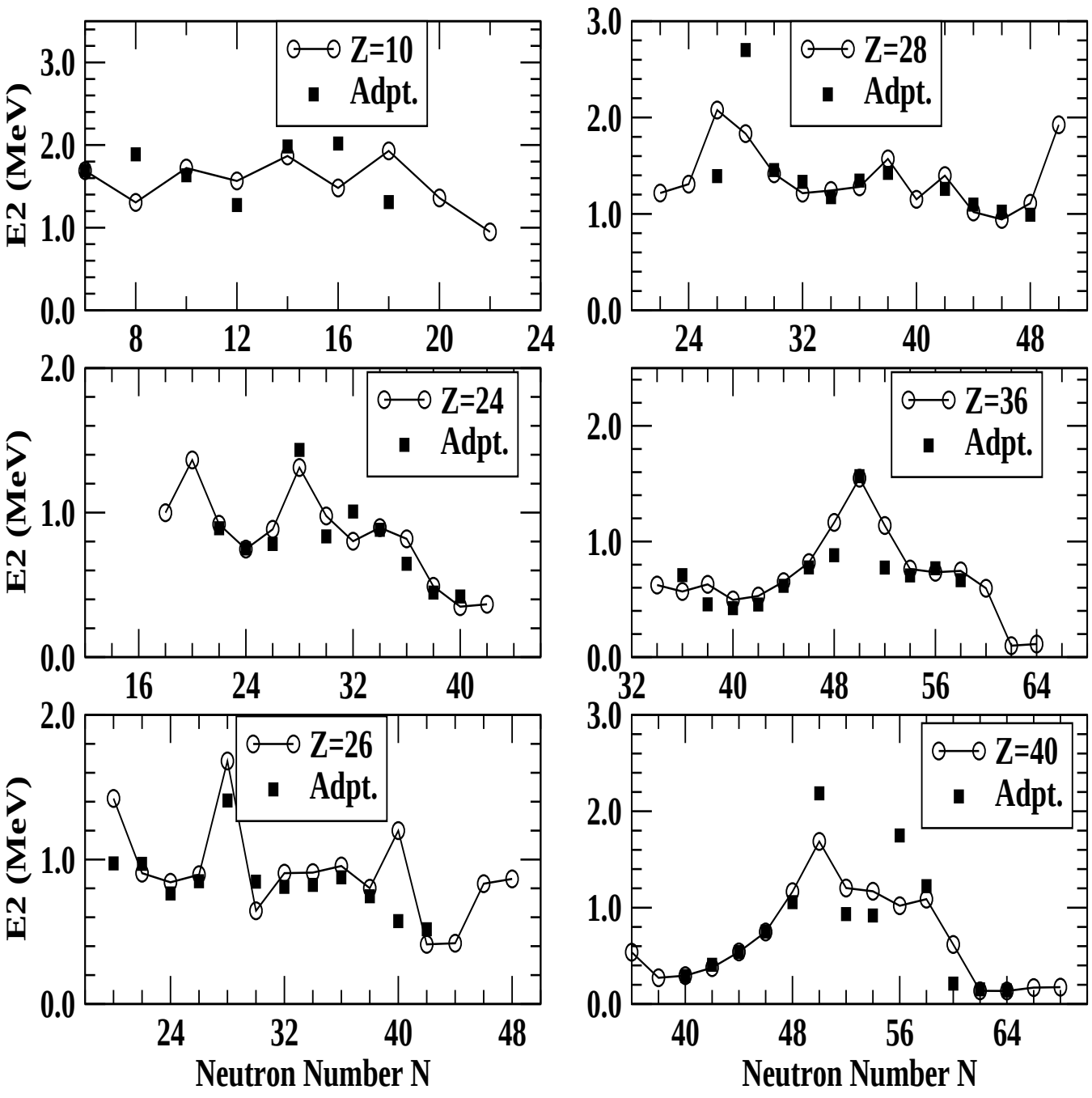

Figure 11: Similar to Fig. 2 but for the values of the excitation energy E2 (see text) for the series Z=10,24, 26, 28,36 and 40. However adopted data are shown without uncertainties as these values are very small.

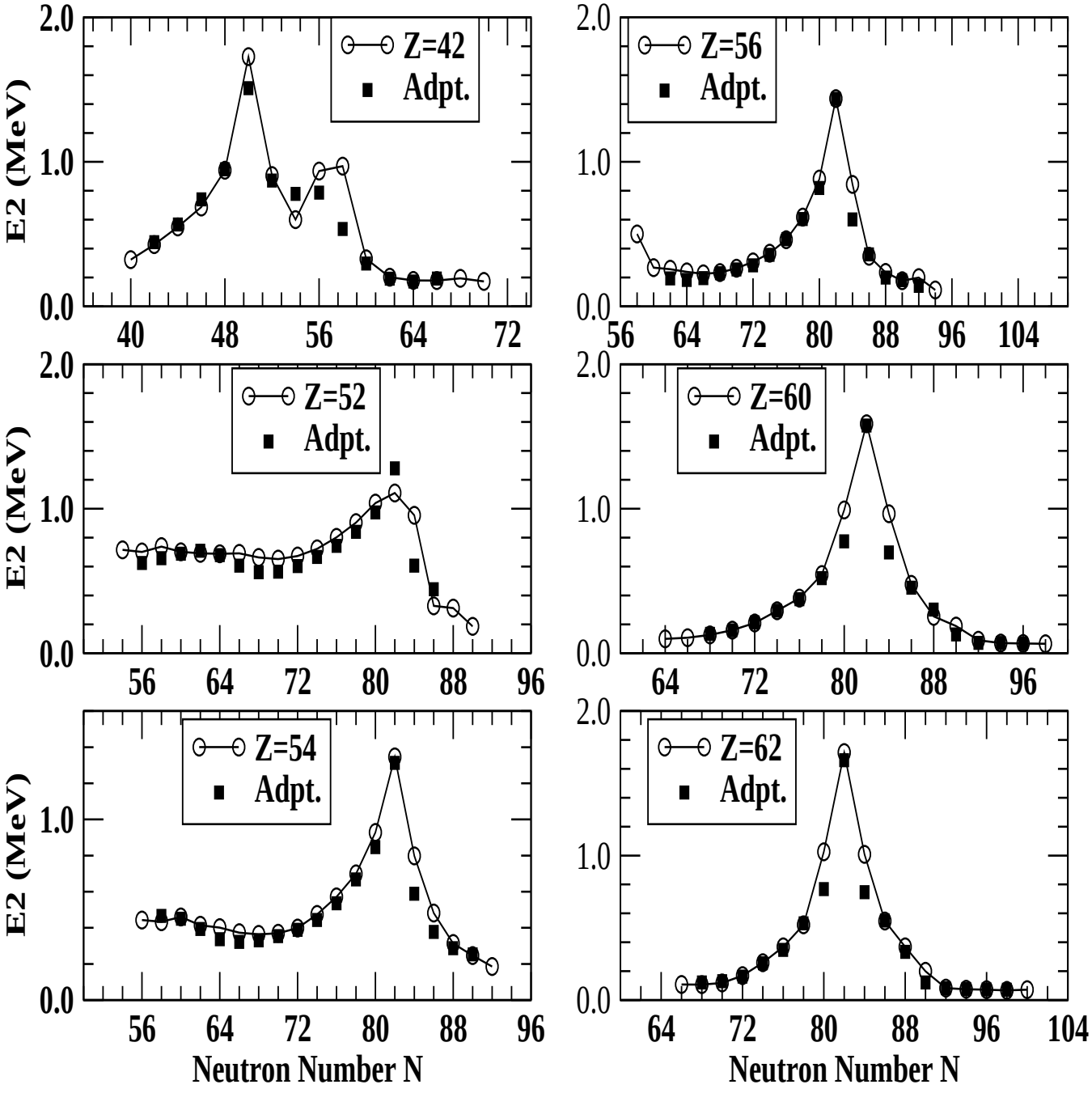

Figure 12: Similar to Fig. 11 but for the values of the excitation energy E2 (see text) for the series Z=42, 52, 54, 56, 60 and 62.

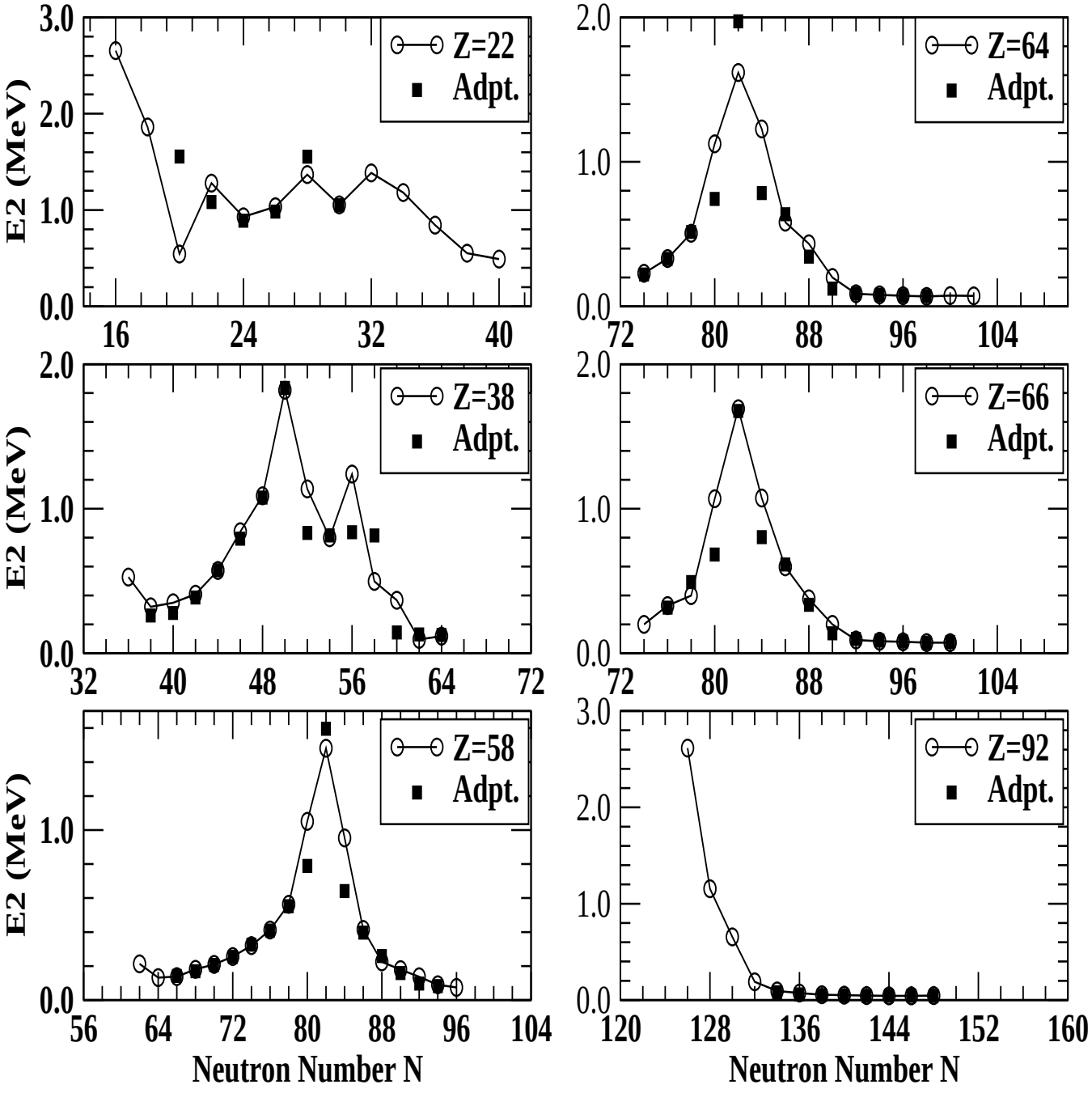

Figure 13: Similar to Figs. 11 and 12 but for the values of the excitation energy E2 (see text) for the series Z=22, 38, 58, 64, 66 and 92.

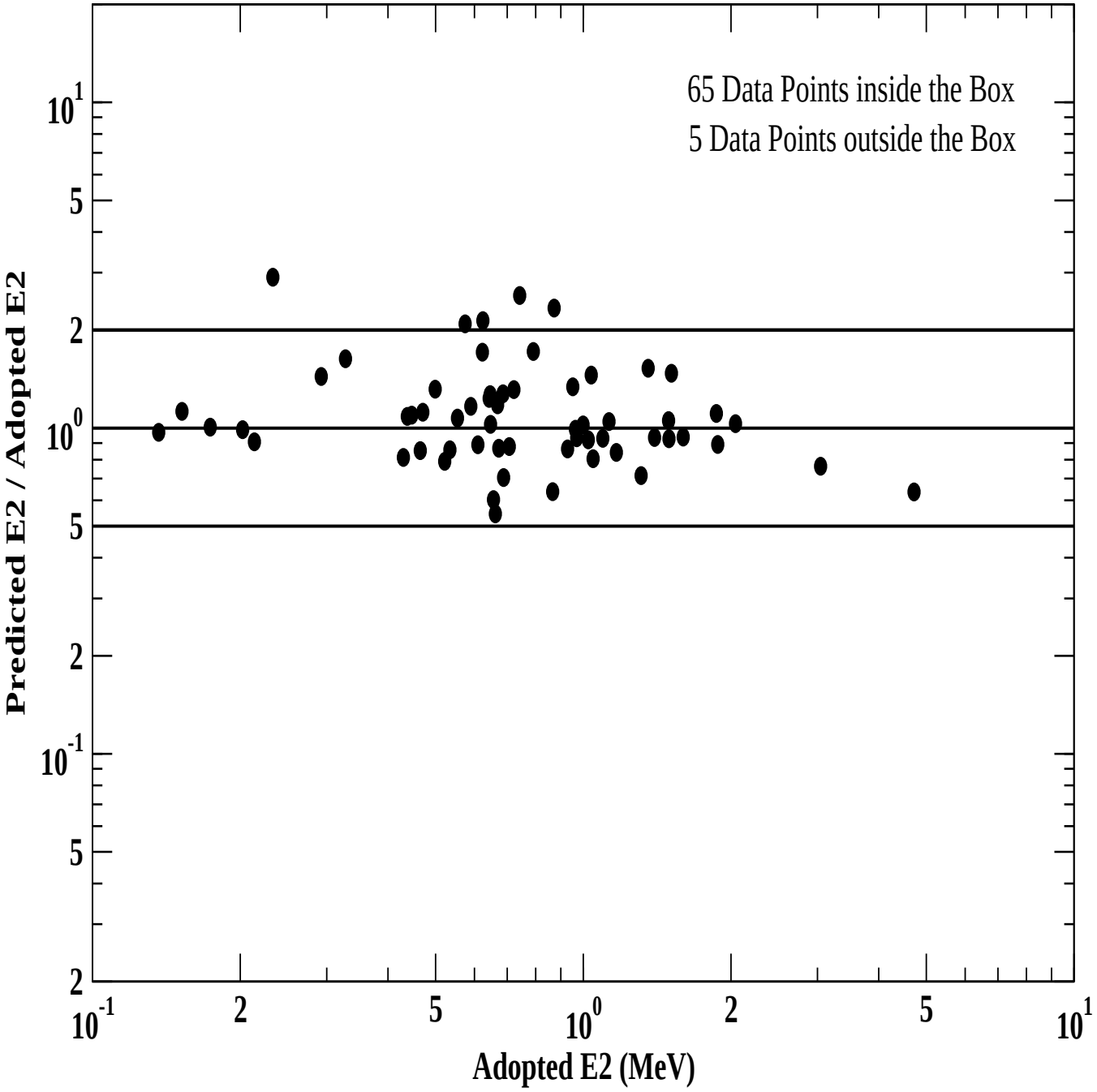

Figure 14: Comparison between the model predictions for the excitation energy $E2$ with the latest adopted experimental data [38] (see text) plotted here in the form of their ratio versus those of the adopted experimental data. The data points lying inside the box indicate the degree of agreement within a factor of two.

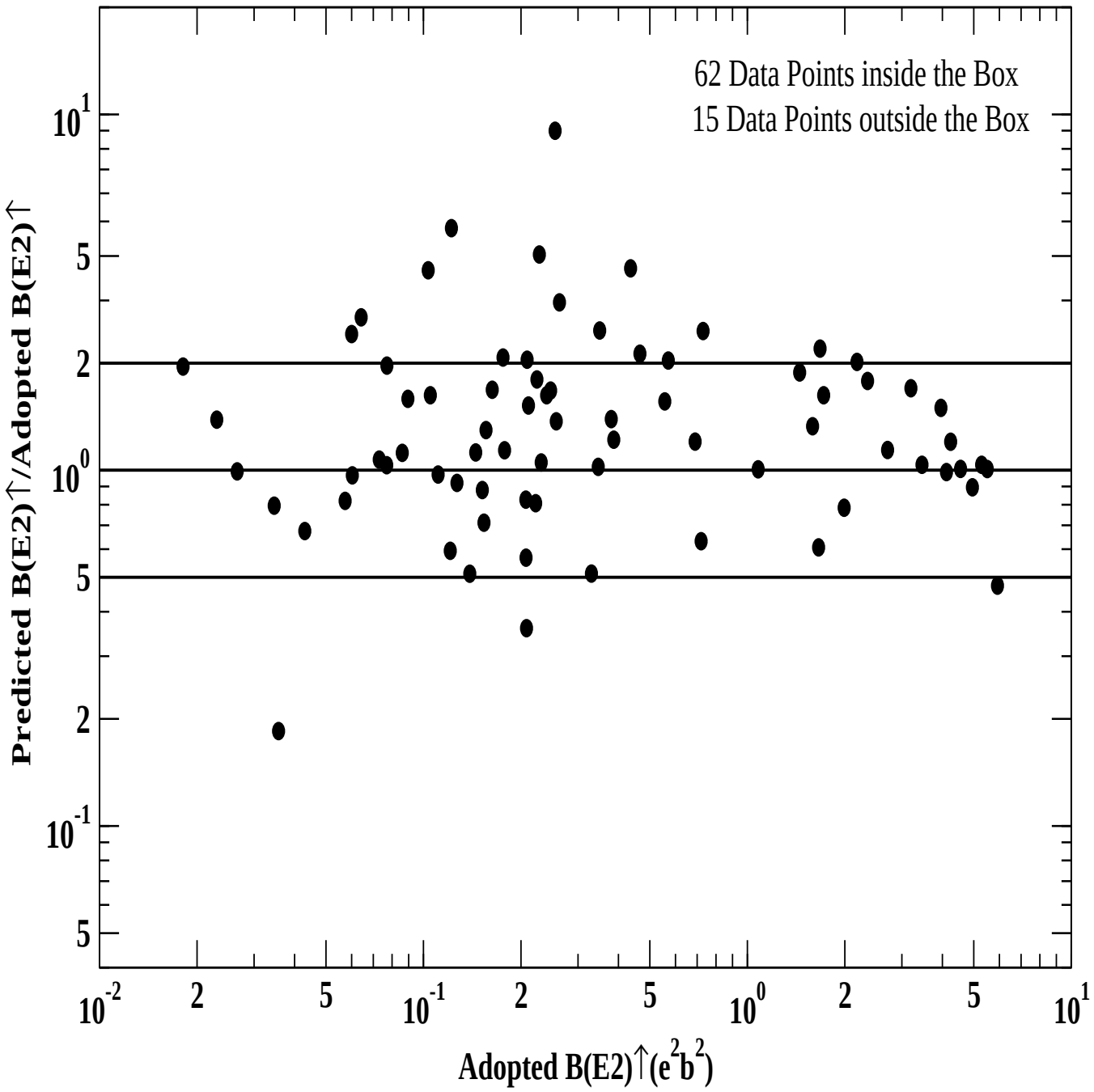

Figure 15: Same as Fig. 13 but for $B(E2)\uparrow$ compared with with the latest adopted experimental data[38] (see text). The data points lying inside the box indicate the degree of agreement within a factor of two.

Table 1. Predicted E2 & B(E2)↑ Values and the Corresponding Calculated Deformation Parameters (See Text)

A	N	$E2$	$B(E2)\uparrow$	β_2	$\beta_2/\beta_{2(sp)}$	Q_0	A	N	$E2$	$B(E2)\uparrow$	β_2	$\beta_2/\beta_{2(sp)}$	Q_0
$Z=8$ (O)							$Z=20$ (Ca)						
12	4	5.505	0.010	0.701	3.536	0.320	50	30	1.075	0.037	0.206	2.594	0.608
14	6	4.529	0.006	0.497	2.507	0.252	52	32	1.079	0.032	0.186	2.341	0.564
24	16	3.005	0.014	0.513	2.591	0.372	54	34	2.108	0.366	0.616	7.766	1.917
$Z=10$ (Ne)							$Z=22$ (Ti)						
30	20	1.360	0.038	0.591	3.729	0.622	38	16	2.655	0.092	0.355	4.924	0.962
32	22	0.948	0.048	0.632	3.988	0.695	40	18	1.862	0.080	0.320	4.440	0.897
$Z=12$ (Mg)							52	30	1.053	0.058	0.229	3.180	0.766
18	6	1.910	0.027	0.579	4.382	0.520	54	32	1.386	0.007	0.075	1.043	0.258
20	8	1.500	0.030	0.569	4.306	0.548	56	34	1.182	0.145	0.344	4.770	1.207
34	22	0.678	0.047	0.501	3.790	0.687	58	36	0.843	0.155	0.347	4.817	1.247
36	24	0.361	0.016	0.284	2.149	0.405	60	38	0.552	0.353	0.513	7.116	1.885
38	26	0.396	0.030	0.371	2.807	0.548	62	40	0.491	0.066	0.216	3.000	0.812
$Z=14$ (Si)							$Z=24$ (Cr)						
22	8	1.928	0.021	0.388	3.427	0.465	42	18	0.999	0.116	0.341	5.166	1.078
24	10	1.673	0.029	0.428	3.781	0.544	44	20	1.364	0.115	0.330	4.993	1.075
40	26	1.022	0.029	0.303	2.672	0.540	60	36	0.818	0.108	0.260	3.933	1.042
42	28	1.894	0.011	0.184	1.621	0.339	62	38	0.490	0.274	0.405	6.134	1.660
44	30	1.679	0.027	0.272	2.406	0.518	64	40	0.349	0.202	0.341	5.158	1.426
$Z=16$ (S)							66	42	0.366				
26	10	2.128	0.029	0.354	3.573	0.542	$Z=26$ (Fe)						
28	12	2.228	0.035	0.371	3.744	0.597	46	20	1.422	0.080	0.246	4.032	0.895
46	30	1.275	0.040	0.282	2.848	0.632	46	20	1.422	0.080	0.246	4.032	0.895
48	32	1.234	0.049	0.304	3.072	0.701	48	22	0.905	0.060	0.208	3.414	0.779
$Z=18$ (Ar)							50	24	0.842	0.179	0.349	5.722	1.342
30	12	2.057	0.029	0.283	3.208	0.535	52	26	0.895	0.092	0.243	3.993	0.961
32	14	2.071	0.026	0.261	2.958	0.515	66	40	1.200	0.134	0.250	4.108	1.159
48	30	1.510	0.028	0.203	2.304	0.526	68	42	0.413	0.203	0.302	4.956	1.427
50	32	2.712	0.037	0.228	2.590	0.607	70	44	0.421				
$Z=20$ (Ca)							72	46	0.833				
36	16	2.326	0.011	0.138	1.741	0.328	74	48	0.866				

Table 1. Predicted E2 & B(E2)↑ Values and the Corresponding Calculated Deformation Parameters (See Text)

A	N	$E2$	$B(E2)\uparrow$	β_2	$\beta_2/\beta_{2(sp)}$	Q_0	A	N	$E2$	$B(E2)\uparrow$	β_2	$\beta_2/\beta_{2(sp)}$	Q_0
$Z = 28$ (Ni)							$Z = 36$ (Kr)						
50	22	1.217					70	34	0.624	0.913	0.455	10.323	3.030
52	24	1.308	0.148	0.287	5.070	1.221	72	36	0.567	0.991	0.465	10.552	3.156
70	42	1.397	0.096	0.190	3.351	0.983	88	52	1.138	0.142	0.154	3.496	1.195
72	44	1.020	0.225	0.285	5.027	1.503	90	54	0.762	0.109	0.133	3.022	1.049
74	46	0.942	0.173	0.245	4.326	1.318	92	56	0.734	0.118	0.136	3.089	1.088
78	50	1.924					94	58	0.746	0.414	0.251	5.708	2.039
$Z = 30$ (Zn)							96	60	0.595	1.609	0.489	11.103	4.022
54	24	1.329	0.096	0.210	3.971	0.980	98	62	0.099				
56	26	0.277	0.080	0.187	3.544	0.896	100	64	0.113				
58	28	2.070	0.026	0.105	1.994	0.516	$Z = 38$ (Sr)						
60	30	1.275	0.095	0.195	3.690	0.977	74	36	0.527	1.236	0.483	11.573	3.525
60	30	1.275	0.095	0.195	3.690	0.977	76	38	0.321	1.086	0.445	10.660	3.305
76	46	0.745	0.163	0.218	4.125	1.279	102	64	0.118	1.319	0.403	9.652	3.641
78	48	0.800	0.080	0.150	2.834	0.894	104	66	0.121				
80	50	1.573	0.078	0.146	2.764	0.887	$Z = 40$ (Zr)						
82	52	1.638	0.085	0.150	2.838	0.925	76	36	0.538				
$Z = 32$ (Ge)							78	38	0.272	1.051	0.408	10.304	3.251
62	30	0.956	0.048	0.127	2.572	0.696	80	40	0.294	1.042	0.400	10.089	3.237
64	32	0.923	0.075	0.155	3.137	0.867	98	58	1.088	0.463	0.233	5.873	2.157
78	46	0.585	0.179	0.211	4.256	1.343	104	64	0.136	1.561	0.411	10.367	3.961
80	48	0.828	0.071	0.131	2.635	0.845	106	66	0.171	1.980	0.457	11.526	4.461
82	50	1.414	0.072	0.129	2.605	0.850	108	68	0.175	1.961	0.449	11.332	4.441
84	52	1.334	0.097	0.148	2.980	0.987	$Z = 42$ (Mo)						
$Z = 34$ (Se)							82	40	0.323	1.575	0.460	12.200	3.979
64	30	0.856	0.263	0.274	5.878	1.625	84	42	0.427	1.451	0.435	11.524	3.819
66	32	0.802	0.289	0.282	6.043	1.705	86	44	0.550	0.759	0.310	8.206	2.762
68	34	0.889	0.321	0.291	6.236	1.795	88	46	0.688	0.066	0.090	2.386	0.816
84	50	1.234	0.171	0.184	3.950	1.309	90	48	0.942	0.318	0.194	5.149	1.787
86	52	1.182	0.187	0.190	4.070	1.370	110	68	0.194	1.650	0.388	10.268	4.073
88	54	0.625	0.054	0.101	2.161	0.739	112	70	0.173	1.769	0.396	10.503	4.217
90	56	0.823	0.124	0.150	3.219	1.117	$Z = 44$ (Ru)						
92	58	0.461					86	42	0.490				

Table 1. Predicted E2 & B(E2)↑ Values and the Corresponding Calculated Deformation Parameters (See Text)

A	N	$E2$	$B(E2)\uparrow$	β_2	$\beta_2/\beta_{2(sp)}$	Q_0	A	N	$E2$	$B(E2)\uparrow$	β_2	$\beta_2/\beta_{2(sp)}$	Q_0
$Z = 44$ (Ru)							$Z = 50$ (Sn)						
92	48	0.906	0.380	0.200	5.547	1.953	126	76	1.046	0.117	0.079	2.496	1.084
94	50	1.390	0.141	0.120	3.333	1.191	128	78	1.101	0.152	0.089	2.814	1.235
114	70	0.260	1.337	0.325	9.024	3.666	130	80	1.276	0.032	0.040	1.277	0.566
116	72	0.421	1.058	0.286	7.935	3.261	136	86	0.485				
118	74	0.535					$Z = 52$ (Te)						
$Z = 46$ (Pd)							106	54	0.715				
90	44	0.522					108	56	0.701	0.471	0.169	5.555	2.177
92	46	0.685					110	58	0.738	0.605	0.189	6.215	2.465
96	50	1.315	0.011	0.032	0.926	0.336	112	60	0.702	0.835	0.220	7.215	2.897
98	52	0.957	0.096	0.092	2.672	0.981	114	62	0.691	0.868	0.222	7.272	2.954
100	54	0.676	0.354	0.175	5.069	1.887	116	64	0.688	0.931	0.227	7.445	3.060
118	72	0.383	0.500	0.186	5.393	2.242	118	66	0.691	1.159	0.250	8.211	3.413
120	74	0.476	0.710	0.219	6.355	2.672	132	80	1.039	0.171	0.089	2.928	1.312
122	76	0.657					134	82	1.109	0.377	0.131	4.303	1.947
124	78	0.688					136	84	0.954	0.584	0.162	5.304	2.424
126	80	0.875					138	86	0.328	0.633	0.167	5.466	2.522
128	82	0.937					140	88	0.312	1.229	0.230	7.545	3.515
							142	90	0.186				
$Z = 48$ (Cd)							$Z = 54$ (Xe)						
96	48	0.770					110	56	0.443	0.346	0.138	4.701	1.865
100	52	1.055	0.169	0.116	3.501	1.303	112	58	0.434	0.669	0.190	6.458	2.593
102	54	0.820	0.352	0.165	4.990	1.882	138	84	0.798	0.529	0.147	4.997	2.306
124	76	0.719	0.864	0.227	6.860	2.948	142	88	0.313	0.830	0.180	6.142	2.889
126	78	0.731	0.779	0.213	6.445	2.799	144	90	0.246	1.797	0.263	8.953	4.250
128	80	0.804					146	92	0.186				
130	82	0.720					$Z = 56$ (Ba)						
$Z = 50$ (Sn)							114	58	0.501	0.373	0.135	4.768	1.937
100	50	1.862					116	60	0.268	0.653	0.177	6.236	2.563
104	54	1.252	0.365	0.159	5.011	1.915	118	62	0.257	1.037	0.220	7.766	3.228
106	56	1.071	0.427	0.170	5.354	2.072	120	64	0.239	2.351	0.327	11.565	4.862
108	58	1.108	0.403	0.163	5.136	2.013	148	92	0.199	3.160	0.330	11.658	5.636
110	60	1.115	0.243	0.125	3.939	1.563	150	94	0.113	2.524	0.292	10.326	5.037

Table 1. Predicted E2 & B(E2)↑ Values and the Corresponding Calculated Deformation Parameters (See Text)

A	N	$E2$	$B(E2)\uparrow$	β_2	$\beta_2/\beta_{2(sp)}$	Q_0	A	N	$E2$	$B(E2)\uparrow$	β_2	$\beta_2/\beta_{2(sp)}$	Q_0
$Z = 58$ (Ce)							$Z = 64$ (Gd)						
120	62	0.213	3.032	0.359	13.132	5.521	140	76	0.331	3.074	0.296	11.931	5.559
122	64	0.132	4.370	0.426	15.594	6.628	142	78	0.506	0.241	0.082	3.313	1.558
142	84	0.954	0.394	0.116	4.234	1.991	144	80	1.125	0.250	0.083	3.341	1.586
144	86	0.415	0.863	0.170	6.205	2.945	146	82	1.618	0.101	0.052	2.107	1.010
152	94	0.090	2.804	0.295	10.789	5.310	148	84	1.228	0.920	0.156	6.292	3.042
154	96	0.074	2.011	0.248	9.056	4.496	150	86	0.583	0.997	0.161	6.490	3.166
$Z = 60$ (Nd)							162	98	0.069	5.547	0.360	14.543	7.468
124	64	0.099	5.634	0.463	17.516	7.526	164	100	0.075	5.479	0.355	14.335	7.421
126	66	0.107	4.988	0.431	16.306	7.082	166	102	0.073	5.728	0.360	14.539	7.588
128	68	0.127	4.392	0.400	15.141	6.645	168	104	0.065				
136	76	0.381	1.008	0.184	6.965	3.183	$Z = 66$ (Dy)						
138	78	0.544	1.322	0.209	7.901	3.646	140	74	0.200				
140	80	0.991	0.455	0.121	4.590	2.138	150	84	1.074	0.241	0.077	3.193	1.558
154	94	0.070	4.187	0.345	13.069	6.488	166	100	0.073	5.560	0.344	14.325	7.476
156	96	0.067	5.011	0.374	14.174	7.098	168	102	0.075	5.694	0.345	14.381	7.566
158	98	0.065					170	104	0.072	5.542	0.338	14.076	7.464
$Z = 62$ (Sm)							$Z = 68$ (Er)						
128	66	0.108					142	74	0.334				
130	68	0.107	5.087	0.412	16.127	7.151	146	78	0.431				
132	70	0.119	4.811	0.397	15.525	6.955	152	84	1.029	0.564	0.113	4.839	2.382
140	78	0.521	0.862	0.162	6.319	2.944	154	86	0.581	0.512	0.106	4.568	2.268
146	84	1.008	0.390	0.106	4.132	1.980	172	104	0.076	5.705	0.330	14.170	7.573
156	94	0.075	4.844	0.356	13.936	6.978	174	106	0.084	4.179	0.281	12.036	6.482
158	96	0.072	5.431	0.374	14.631	7.389	176	108	0.085	3.987	0.272	11.667	6.331
160	98	0.067	5.745	0.382	14.923	7.600	$Z = 70$ (Yb)						
162	100	0.072	5.594	0.373	14.604	7.499	150	80	1.454				
							154	84	0.865	3.184	0.258	11.396	5.657
$Z = 64$ (Gd)							156	86	0.524	2.010	0.203	8.978	4.496
132	68	0.116					178	108	0.084	5.016	0.294	12.987	7.101
134	70	0.099					180	110	0.091	4.176	0.266	11.763	6.480
136	72	0.123					182	112	0.119	1.219	0.143	6.307	3.500
138	74	0.229	4.394	0.357	14.403	6.646							

Table 1. Predicted E2 & B(E2)↑ Values and the Corresponding Calculated Deformation Parameters (See Text)

A	N	$E2$	$B(E2)\uparrow$	β_2	$\beta_2/\beta_{2(sp)}$	Q_0	A	N	$E2$	$B(E2)\uparrow$	β_2	$\beta_2/\beta_{2(sp)}$	Q_0
$Z = 72$ (Hf)							$Z = 78$ (Pt)						
152	80	1.460					176	98	0.287	2.580	0.191	9.385	5.093
158	86	0.633	1.120	0.146	6.645	3.356	178	100	0.182	5.098	0.266	13.093	7.159
160	88	0.402	0.601	0.106	4.827	2.458	180	102	0.187	4.810	0.257	12.623	6.954
182	110	0.108	4.062	0.254	11.515	6.390	182	104	0.183	3.583	0.220	10.816	6.002
184	112	0.113	2.982	0.216	9.794	5.475	200	122	0.489	0.737	0.094	4.607	2.723
186	114	0.135	2.537	0.197	8.970	5.050	202	124	0.459	0.130	0.039	1.919	1.141
188	116	0.297					204	126	2.037	0.457	0.073	3.581	2.144
$Z = 74$ (W)							$Z = 80$ (Hg)						
156	82	2.301					170	90	0.681				
158	84	1.327					172	92	0.583				
160	86	0.542					174	94	0.664				
164	90	0.339	0.400	0.083	3.873	2.005	180	100	0.418	2.729	0.188	9.508	5.238
166	92	0.256	1.714	0.170	7.953	4.151	182	102	0.338	3.684	0.217	10.967	6.086
176	102	0.110	4.433	0.264	12.301	6.676	188	108	0.414	2.793	0.185	9.345	5.299
178	104	0.105	4.591	0.266	12.425	6.794	190	110	0.464	4.085	0.222	11.221	6.408
188	114	0.176	3.089	0.211	9.827	5.573	$Z = 80$ (Hg)						
190	116	0.173	1.663	0.153	7.160	4.089	192	112	0.498	1.623	0.139	7.023	4.039
192	118	0.220	1.206	0.130	6.055	3.482	194	114	0.506	1.521	0.134	6.753	3.910
194	120	0.421					206	126	0.638	0.622	0.082	4.150	2.501
$Z = 76$ (Os)							208	128	0.788	0.418	0.067	3.381	2.051
162	86	0.620					210	130	0.793	0.082	0.029	1.487	0.908
168	92	0.356	1.393	0.148	7.114	3.742	212	132	0.866				
170	94	0.290	3.025	0.217	10.399	5.514	$Z = 82$ (Pb)						
176	100	0.113	5.438	0.284	13.624	7.394	178	96	0.695				
178	102	0.128	4.071	0.244	11.700	6.397	180	98	0.984				
194	118	0.279	1.686	0.148	7.110	4.117	186	104	0.614	2.933	0.186	9.645	5.430
196	120	0.305	0.599	0.088	4.207	2.453	188	106	0.665	2.293	0.164	8.467	4.801
198	122	0.397	0.243	0.056	2.663	1.563	190	108	0.693	1.120	0.114	5.876	3.356
$Z = 78$ (Pt)							192	110	0.772	3.963	0.212	10.976	6.312
166	88	0.699					194	112	0.881	1.805	0.142	7.357	4.260
172	94	0.434	1.382	0.142	6.975	3.727	196	114	0.947	1.829	0.142	7.355	4.288
174	96	0.359	1.229	0.133	6.527	3.515	198	116	0.947	1.411	0.124	6.415	3.766

Table 1. Predicted E2 & B(E2)↑ Values and the Corresponding Calculated Deformation Parameters (See Text)

A	N	$E2$	$B(E2)\uparrow$	β_2	$\beta_2/\beta_{2(sp)}$	Q_0	A	N	$E2$	$B(E2)\uparrow$	β_2	$\beta_2/\beta_{2(sp)}$	Q_0
$Z = 82$ (Pb)							$Z = 88$ (Ra)						
200	118	0.919	1.217	0.114	5.918	3.498	236	148	0.037	9.642	0.269	14.920	9.845
202	120	0.833	0.618	0.081	4.190	2.492	$Z = 90$ (Th)						
212	130	0.671	0.064	0.025	1.302	0.800	208	118	0.423				
216	134	0.732					210	120	0.419				
$Z = 84$ (Po)							212	122	0.581				
184	100	1.138					214	124	1.065				
186	102	0.767					218	128	0.886	0.551	0.066	3.759	2.353
188	104	0.601					220	130	0.488	0.782	0.078	4.454	2.805
190	106	0.677					224	134	0.112	5.927	0.213	12.111	7.719
196	112	0.557	2.112	0.149	7.904	4.608	236	146	0.048	9.222	0.257	14.591	9.629
198	114	0.636	2.184	0.151	7.983	4.686	238	148	0.044	10.482	0.272	15.469	10.265
200	116	0.716	1.719	0.133	7.035	4.158	$Z = 92$ (U)						
202	118	0.741	2.108	0.146	7.739	4.604	218	126	2.615				
204	120	0.744	0.810	0.090	4.766	2.854	220	128	1.155				
206	122	0.763	0.258	0.050	2.673	1.611	222	130	0.656				
208	124	0.775	0.196	0.044	2.315	1.404	224	132	0.190	4.238	0.176	10.242	6.527
212	128	0.820	0.033	0.018	0.932	0.572	226	134	0.094	7.505	0.233	13.548	8.686
220	136	0.392					228	136	0.073	9.002	0.254	14.752	9.513
$Z = 86$ (Rn)							240	148	0.046	12.691	0.292	16.927	11.295
194	108	0.196					242	150	0.047	13.836	0.303	17.576	11.794
196	110	0.187					244	152	0.040	14.057	0.304	17.619	11.888
224	138	0.147	4.116	0.186	10.093	6.433	246	154	0.040	15.872	0.321	18.620	12.632
226	140	0.056	5.361	0.211	11.451	7.341	$Z = 94$ (Pu)						
228	142	0.046					228	134	0.114				
$Z = 88$ (Ra)							230	136	0.071	8.664	0.243	14.388	9.333
200	112	0.225					232	138	0.059	9.461	0.252	14.948	9.753
202	114	0.349					234	140	0.050	9.213	0.247	14.667	9.624
204	116	0.439					236	142	0.042	11.257	0.272	16.121	10.638
220	132	0.279	5.062	0.204	11.329	7.134	246	152	0.046	13.915	0.294	17.434	11.827
230	142	0.057	7.909	0.248	13.746	8.917	248	154	0.043	15.366	0.307	18.222	12.429
232	144	0.056	6.472	0.223	12.364	8.066	$Z = 96$ (Cm)						
234	146	0.053	7.747	0.242	13.449	8.825	236	140	0.028	12.032	0.275	16.667	10.998

Table 1. Predicted E2 & B(E2)↑ Values and the Corresponding Calculated Deformation Parameters (See Text)

A	N	$E2$	$B(E2)\uparrow$	β_2	$\beta_2/\beta_{2(sp)}$	Q_0	A	N	$E2$	$B(E2)\uparrow$	β_2	$\beta_2/\beta_{2(sp)}$	Q_0
$Z = 96$ (Cm)													
238	142	0.040	15.228	0.308	18.645	12.373							
242	146	0.041	13.970	0.292	17.661	11.851							
250	154	0.047	16.004	0.305	18.498	12.684							
252	156	0.042	15.778	0.302	18.269	12.595							
$Z = 98$ (Cf)													
236	138	0.020	7.351	0.211	13.028	8.597							
238	140	0.023	12.734	0.276	17.050	11.314							
240	142	0.031	16.918	0.316	19.543	13.041							
242	144	0.035	15.093	0.297	18.357	12.318							
244	146	0.042	13.743	0.282	17.421	11.754							
246	148	0.042	14.559	0.288	17.834	12.098							
248	150	0.043	15.807	0.299	18.482	12.606							
254	156	0.049											
$Z = 100$ (Fm)													
246	146	0.041	12.806	0.265	16.725	11.347							
248	148	0.045	12.973	0.265	16.743	11.420							
250	150	0.044	15.834	0.292	18.399	12.617							
252	152	0.042	15.241	0.285	17.955	12.378							